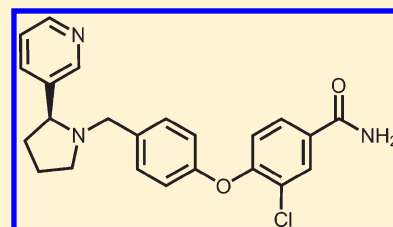


Discovery of Aminobenzyloxyarylamides as  $\kappa$  Opioid Receptor Selective Antagonists: Application to Preclinical Development of a  $\kappa$  Opioid Receptor Antagonist Receptor Occupancy TracerCharles H. Mitch,<sup>\*,†</sup> Steven J. Quimby,<sup>†</sup> Nuria Diaz,<sup>‡</sup> Concepcion Pedregal,<sup>‡</sup> Marta G. de la Torre,<sup>‡</sup> Alma Jimenez,<sup>‡</sup> Qing Shi,<sup>†</sup> Emily J. Canada,<sup>†</sup> Steven D. Kahl,<sup>†</sup> Michael A. Statnick,<sup>†</sup> David L. McKinzie,<sup>†</sup> Dana R. Benesh,<sup>†</sup> Karen S. Rash,<sup>†</sup> and Vanessa N. Barth<sup>†</sup><sup>†</sup>Lilly Research Laboratories, Lilly Corporate Center, Eli Lilly and Company, Indianapolis, Indiana 46285-0150, United States<sup>‡</sup>Lilly SA, Avenida de la Industria 30, 28108-Alcobendas, Madrid, Spain

## S Supporting Information

**ABSTRACT:** Arylphenylpyrrolidinylmethylphenoxybenzamides were found to have high affinity and selectivity for  $\kappa$  opioid receptors. On the basis of receptor binding assays in Chinese hamster ovary (CHO) cells expressing cloned human opioid receptors, (S)-3-fluoro-4-(4-((2-(3-fluorophenyl)pyrrolidin-1-yl)methyl)phenoxy)benzamide (**25**) had a  $K_i = 0.565$  nM for  $\kappa$  opioid receptor binding while having a  $K_i = 35.8$  nM for  $\mu$  opioid receptors and a  $K_i = 211$  nM for  $\delta$  opioid receptor binding. Compound **25** was also a potent antagonist of  $\kappa$  opioid receptors when tested in vitro using a [<sup>35</sup>S]-guanosine 5'-O-[3-thiotriphosphate] ([<sup>35</sup>S]GTP- $\gamma$ -S) functional assay in CHO cells expressing cloned human opioid receptors. Compounds were also evaluated for potential use as receptor occupancy tracers. Tracer evaluation was done in vivo, using liquid chromatography-tandem mass spectrometry (LC/MS/MS) methods, precluding the need for radiolabeling. (S)-3-Chloro-4-(4-((2-(pyridine-3-yl)pyrrolidin-1-yl)methyl)phenoxy)benzamide (**18**) was found to have favorable properties for a tracer for receptor occupancy, including good specific versus nonspecific binding and good brain uptake.



## INTRODUCTION

Kappa opioid receptors were first proposed by Martin et al. in 1976 based on observations of differing pharmacological responses when comparing effects of ketocyclazocine and morphine in a spinal dog model.<sup>1</sup> Goldstein and Chavkin characterized a 13-amino acid peptide as an endogenous ligand for the  $\kappa$  opioid receptor.<sup>2a</sup> Subsequently, a family of related peptides of varying amino acid length and composition has been identified and these are known as dynorphins.<sup>2b</sup> Considerable interest in the potential of  $\kappa$  agonists as a new type of analgesic followed the report by Szmuszkovics of U50,488 being highly potent and efficacious in preclinical pain models and that this analgesia was mediated through  $\kappa$  opioid receptors and not the  $\mu$  opioid receptor associated with morphine analgesia.<sup>3</sup> This interest was tempered by the report of Pfeifer and Herz et al. that the  $\kappa$  agonist MR2034 produced psychotomimetic and dysphoric subjective effects in normal human volunteers.<sup>4</sup> A potential mechanistic understanding of these clinical findings comes from the work of Shippenberg et al. using microdialysis to study neurotransmitter release.<sup>5</sup>

A single gene for the  $\kappa$  opioid receptor has been cloned, as reported by Yasuda et al. in 1993.<sup>6</sup> While numerous proposals for subtypes of  $\kappa$  opioid receptors have appeared, only a single gene at the molecular level has been identified to date.<sup>7</sup> Sequence analysis of the  $\kappa$  opioid receptor shows high homology with both  $\mu$  and  $\delta$  opioid receptors, suggestive that finding agonists and antagonists with selectivity for each receptor may be challenging.<sup>8</sup>

Antagonists of  $\kappa$  opioid receptors may have therapeutic potential for a range of diseases and disorders.<sup>9</sup> The psychotomimetic and dysphoric effects associated with  $\kappa$  opioid agonists raises the possibility that  $\kappa$  opioid antagonists may be useful for the treatment of schizophrenia and other psychotic disorders.<sup>10</sup> Potential therapeutic utility in the treatment of affective disorders, such as depression and anxiety, has been proposed based on the activity of  $\kappa$  antagonists in animal models.<sup>11</sup> Clinical antidepressant efficacy reported for buprenorphine has been attributed to the  $\kappa$  antagonist pharmacology associated with this agent.<sup>10</sup> Utility in the treatment of addictive disorders has also been proposed for  $\kappa$  opioid antagonists.<sup>12</sup>

nor-Binaltorphamine **1**, with a structure based on the fusion of two naltrexone related fragments onto a core pyrrole ring, was reported by Portoghese to have potent and selective affinity for  $\kappa$  opioid receptors (Figure 1).<sup>13</sup> Another scaffold type for  $\kappa$  selectivity was JDTic, **2a**, with a structure based on a 3,4-dimethyl-4-(3-hydroxyphenyl)piperidine connected with an N-linked tetrahydroisoquinoline-carboxamide.<sup>14</sup> More recently, azabicyclooctane based  $\kappa$  selective antagonists, as exemplified by **3**, have been disclosed by Brugel and co-workers.<sup>15</sup>

Discovery of selective receptor occupancy tracers can provide important tools for preclinical and clinical characterization of target engagement for the development of new therapeutic

Received: June 17, 2011

Published: September 29, 2011

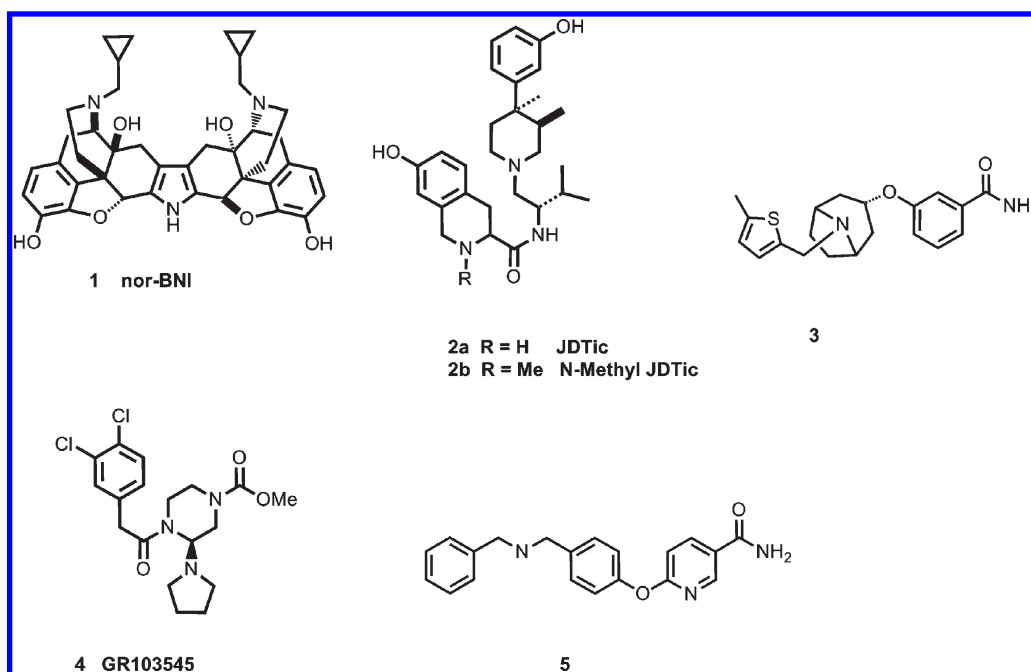
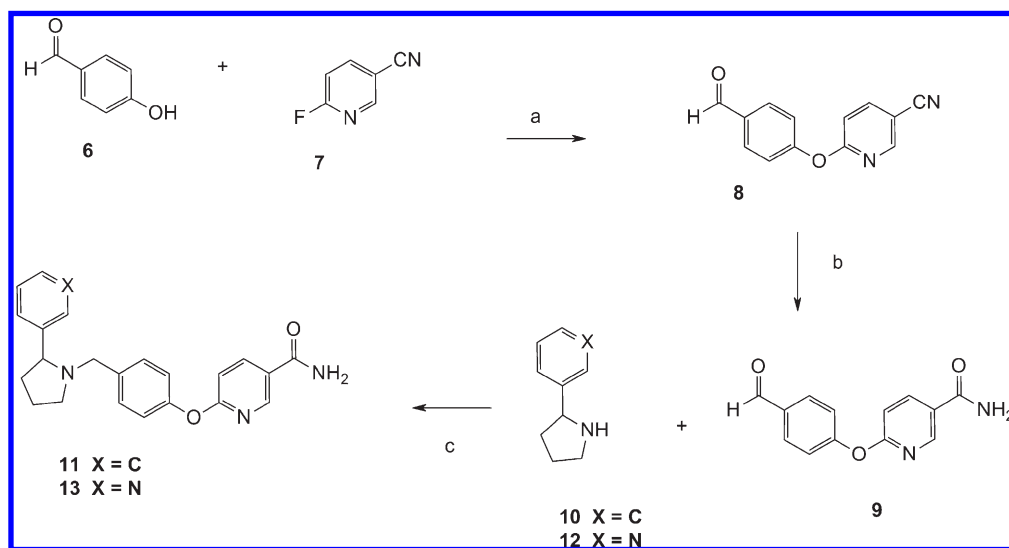


Figure 1

Scheme 1<sup>a</sup>

<sup>a</sup> Reagents and conditions: (a)  $K_2CO_3$ , DMF, 140 °C; (b)  $H_2O_2$ , NaOH; (c)  $NaBH(OAc)_3$ , AcOH, 1,2-DCE.

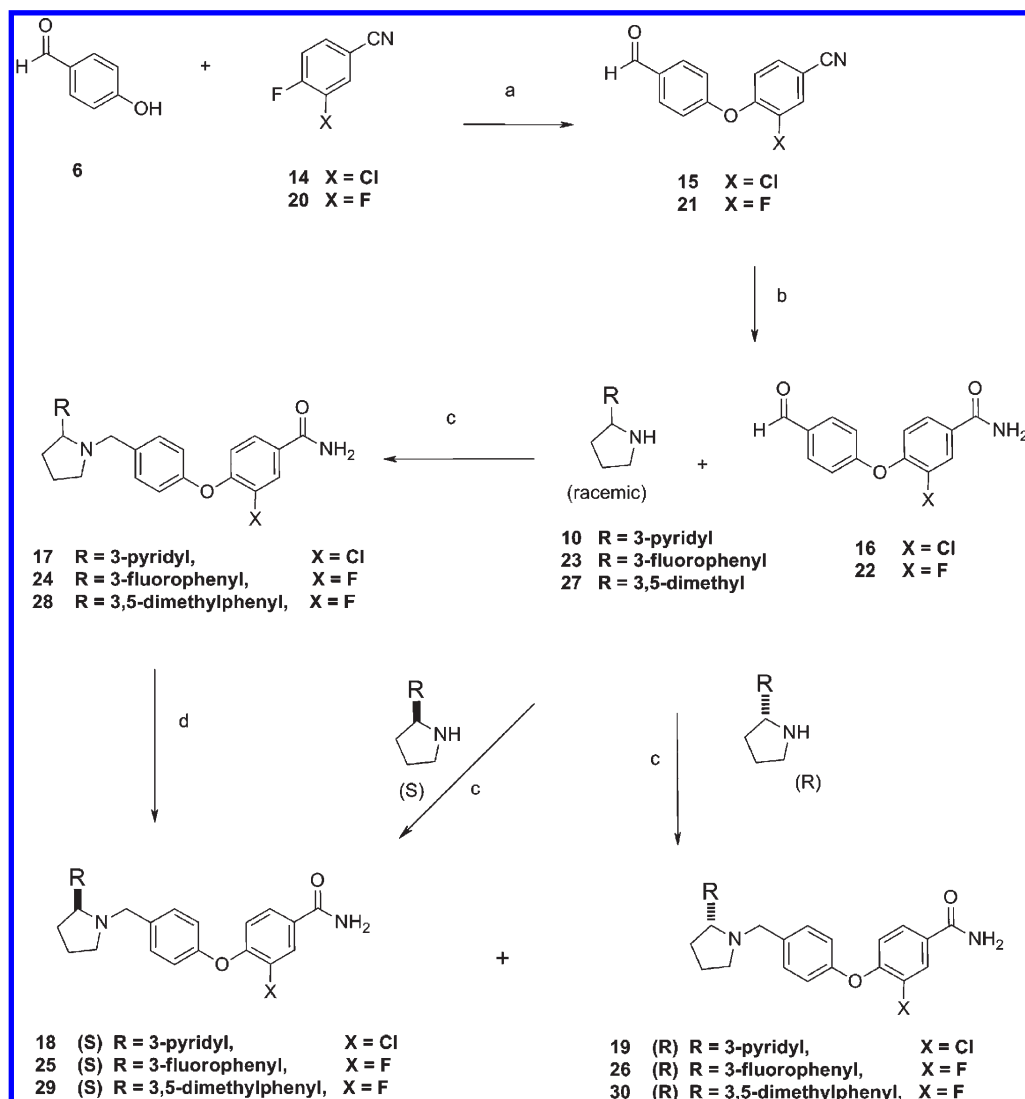
agents. The  $\kappa$  agonist GR103545 (**4**) has been successfully used as a tracer for receptor occupancy studies.<sup>16</sup> The adverse events associated with  $\kappa$  agonist pharmacology may limit the clinical utility of **4** for receptor occupancy studies. Additionally, there may be differences in receptor binding interactions between agonist and antagonist ligands. As a result, there remains considerable interest in finding  $\kappa$  antagonists suitable for use as receptor occupancy tracers.

We have previously disclosed potent but nonselective opioid antagonist activity for a series of aminobenzoyloxyarylamides, as exemplified by **5**. This constituted a novel scaffold for opioid antagonist activity.<sup>17</sup> In this report, we describe details of our

discovery of potent and selective  $\kappa$  antagonists in an aminobenzoyloxyarylamide scaffold. We also describe the evaluation of this new type of  $\kappa$  antagonist for potential use as a receptor occupancy tracer.

## CHEMISTRY

Nicotinamide analogues were prepared as shown in Scheme 1. Reaction of 4-hydroxybenzaldehyde **6**, 6-fluoro-3-pyridinecarboxitrile **7**, and  $K_2CO_3$  in DMF at 100 °C for 2 h gave 6-(4-formylphenoxy)-3-pyridinecarboxitrile **8**. Conversion to 6-(4-formylphenoxy)-3-pyridinecarboxamide **9** was carried out with

Scheme 2<sup>a</sup>

<sup>a</sup> Reagents and conditions: (a) K<sub>2</sub>CO<sub>3</sub>, DMF, 140 °C; (b) H<sub>2</sub>O<sub>2</sub>, NaOH; (c) NaBH(OAc)<sub>3</sub>, AcOH, 1,2-DCE; (d) chiral chromatography.

basic hydrogen peroxide. Reductive amination with 2-phenylpyrrolidine, **10**, utilizing sodium triacetoxy borohydride and acetic acid in 1,2-dichloroethylene, gave racemic 6-[4-[[2-phenylpyrrolidin-1-yl]methyl]phenoxy]pyridine-3-carboxamide **11**.

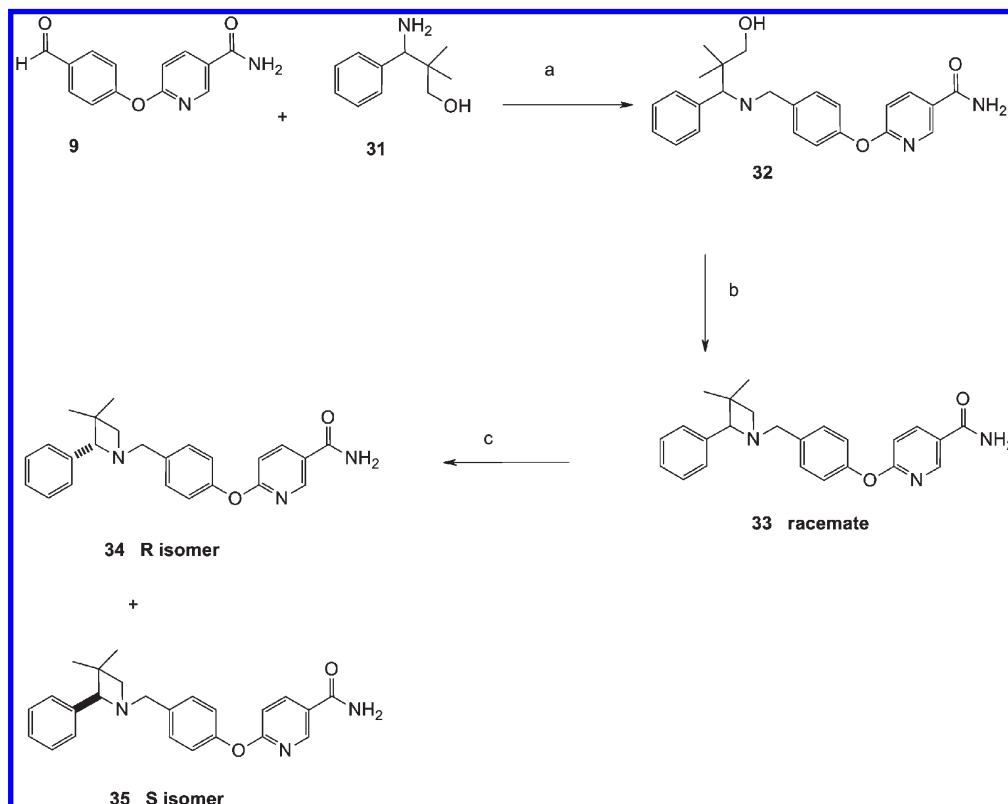
Reductive amination with 3-(2-pyrrolidinyl)-pyridine, **12**, utilizing sodium triacetoxy borohydride and acetic acid in 1,2-dichloroethylene gave racemic 6-[4-[[2-(3-pyridyl)pyrrolidin-1-yl]methyl]phenoxy]pyridine-3-carboxamide **13**.

Halogenated benzamide compounds were prepared by the route shown in Scheme 2. Reaction of 4-hydroxybenzaldehyde **6**, 3-chloro-4-fluorobenzonitrile **14** and K<sub>2</sub>CO<sub>3</sub> in DMF at 100 °C for 2 h afforded 3-fluoro-4-(4-formylphenoxy)benzonitrile **15**. Hydrolysis with basic hydrogen peroxide then gave 3-chloro-4-(4-formylphenoxy)-benzamide **16**. Reductive amination of **16** with racemic 3-(2-pyrrolidinyl)-pyridine, **10**, utilizing sodium triacetoxy borohydride and acetic acid in 1,2-dichloroethylene, gave 3-chloro-4-[4-[[2-(3-pyridyl)pyrrolidin-1-yl]methyl]phenoxy]-benzamide **17** in racemic form. Separation by chiral HPLC then gave enantiomers **18** and **19** in high enantiomeric purity. Absolute configurations for **18** and **19** were established by independently

preparing the respective isomers from 3-(2-pyrrolidinyl)-pyridine already resolved into (S) and (R) enantiomers by chiral chromatography.

Fluorobenzamide analogues were prepared by a similar route. Reaction of 4-hydroxybenzaldehyde **6**, and 3,4-difluorobenzonitrile **20**, followed by hydrolysis with basic hydrogen peroxide, then gave 3-fluoro-4-(4-formylphenoxy)-benzamide **22**. Reductive amination with racemic 2-(3-fluorophenyl)pyrrolidine then gave racemic 3-fluoro-4-[4-[[2-(3-fluorophenyl)pyrrolidin-1-yl]methyl]phenoxy]benzamide **24**. Enantiomers **25** and **26** were then obtained by preparative chiral chromatography of racemic **24**. Reductive amination of aldehyde **22** with (R)-2-(3-fluorophenyl)pyrrolidine produced enantiomer **26**.<sup>18</sup> Enantiomer **25** was correspondingly assigned as having (S) absolute configuration.

Using similar methods, reductive amination of **22** with racemic 2-(3,5-dimethylphenyl)pyrrolidine afforded racemic **28**. Enantiomers **29** and **30** were separated by chiral chromatography. Reductive amination of aldehyde **20** with (S)-2-(3,5-dimethylphenyl)pyrrolidine produced (S)-enantiomer **29**.

Scheme 3<sup>a</sup>

<sup>a</sup> Reagents and conditions: (a) NaCNBH<sub>3</sub>, AcOH, dioxane; (b) bis-(2-methoxyethyl)amino)sulfur trifluoride; (c) chiral chromatography.

Azetidine analogues were prepared by the route shown in Scheme 3. Reductive amination of 6-(4-formylphenoxy)-3-pyridinecarboxamide **9** with  $\gamma$ -amino- $\beta,\beta$ -dimethylbenzenepropanol **31**, using sodium cyanoborohydride and acetic acid in dioxane, gave 6-[4-[(3-hydroxy-2,2-dimethyl-1-phenyl-propyl)amino]-methyl]phenoxy]pyridine-3-carboxamide **32**. Cyclization to form the azetidine ring was carried out with bis-(2-methoxyethyl)amino-sulfur trifluoride to give 6-[4-[(3,3-dimethyl-2-phenyl-azetidin-1-yl)methyl]phenoxy]pyridine-3-carboxamide **33** in racemic form. Separation of enantiomers by chiral chromatography then gave enantiomers **34** and **35**. Assignment of absolute configuration was made by comparison of measured vibrational circular dichroism (VCD) spectra with theoretical VCD spectra calculated from Gaussian B3PW91/6-31G\*\* on the lowest energy conformations determined from Monte Carlo simulations.<sup>19</sup>

## ■ PHARMACOLOGY

Compounds were first evaluated in vitro for receptor binding affinity for  $\kappa$ ,  $\mu$ , and  $\delta$  opioid receptors. Radioligand displacement studies with [<sup>3</sup>H]diprenorphine were carried out using membranes prepared from CHO cells cloned to express human  $\kappa$  and  $\mu$  opioid receptors or HEK293 cells expressing the cloned  $\delta$  opioid receptor.<sup>21</sup> Concentrations causing 50% inhibition (IC<sub>50</sub>) of opioid antagonist radioligand ([<sup>3</sup>H]-diprenorphine) binding were determined from 11 point concentration response curves in assay buffer containing sodium and guanosine diphosphate (GDP). Naltrexone was included as a control at 10  $\mu$ M to define nonspecific binding and was also tested as a comparator molecule

in concentration response curves. Results from in vitro receptor binding studies are shown in Table 1.

The highest affinity and selectivity for  $\kappa$  receptors was found for compound **25**, with  $\kappa$  K<sub>i</sub> = 0.565 nM. This compound showed 63-fold higher affinity for  $\kappa$  receptors than for  $\mu$  receptors and more than 370-fold higher affinity for  $\kappa$  receptors than for  $\delta$  receptors. The corresponding opposite enantiomer, compound **26**, had substantially weaker affinity for  $\kappa$  receptors, with a K<sub>i</sub> = 53.7 nM. Compound **29**, with  $\kappa$  K<sub>i</sub> = 0.949 nM, also showed good affinity and selectivity for  $\kappa$  opioid receptors.

Compounds were evaluated for in vitro antagonist activity, utilizing inhibition of agonist stimulated [<sup>35</sup>S]-guanosine 5'-[3-thiotriphosphate] ([<sup>35</sup>S]GTP- $\gamma$ -S) binding with cloned human opioid receptors expressed in Chinese hamster ovary cells (CHO) cells ( $\mu$  and  $\kappa$ ) or human embryonic kidney 293 (HEK293) cells ( $\delta$ ).<sup>22</sup> First,  $\kappa$  antagonist activity was measured based on blockade of the  $\kappa$  opioid agonist *N*-methyl-*N*-[(5*R*,7*S*,8*S*)-7-(1-pyrrolidinyl)-1-oxaspiro[4.5]dec-8-yl]-benzeneacetamide (U-69,593). Then  $\mu$  antagonism was measured using blockade of the  $\mu$  agonist *L*-tyrosyl-*D*-alanylglycyl-*N*-(2-hydroxyethyl)-*N* $\alpha$ -methyl-*L*-phenylalaninamide (DAMGO). Finally,  $\delta$  antagonism was measured based on inhibition of the  $\delta$  agonist *L*-tyrosyl-3-mercapto-*D*-valylglycyl-*L*-phenylalanyl-3-mercapto-, cyclic (2*S*)-disulfide, *D*-valine (DPDPE). Compounds were tested in functional GTP- $\gamma$ -S binding assays (in the absence or presence of agonist) with scintillation proximity assay (SPA) technology using membranes prepared from CHO cells expressing the cloned human opioid receptor subtypes ( $\kappa$ ,  $\mu$ ) or HEK293 cells expressing cloned human receptor ( $\delta$ ). Opioid

**Table 1. In Vitro Receptor Affinity for  $\kappa$ ,  $\mu$ , and  $\delta$  Opioid Receptors**

compd	$\kappa$ $K_i$ (nM) <sup>a</sup>	$\mu$ $K_i$ (nM) <sup>a</sup>	$\delta$ $K_i$ (nM) <sup>a</sup>	$\mu/\kappa$	$\delta/\kappa$
1	0.153 ± 0.0327	32.4 ± 3.84	6.56 ± 0.704	212	43
2a	0.0591 ± 0.0158	11.5 ± 1.34	188 ± 24.7	87	1730
2b	0.153 ± 0.0192	30.8 ± 4.77	>500	201	>3200
4	0.502 ± 0.101	34.7 ± 6.2	422 ± 6.62	69	841
5	1.78 ± 0.233	2.43 ± 0.373	27.6 ± 2.07	1	16
11	9.21 ± 0.508	232 ± 25.4	>500	25	>50
13	1.49 <sup>b</sup>	39.6 ± 3.69	>500	27	>330
17	0.622 ± 0.0692	31.5 ± 11.7	251 ± 1.6	51	404
18	0.722 ± 0.221	25.8 ± 12.6	153 ± 50.3	36	212
19	44.9 ± 25.3	>500	>500	>11	>11
24	0.617 ± 0.169	41.1 ± 2.17	187 ± 12.9	67	303
25	0.565 ± 0.147	35.8 ± 7.57	211 ± 45.6	63	373
26	53.7 ± 15.8	>500	>500	>9	>9
29	0.949 ± 0.351	22.7 ± 6.34	166 ± 48.0	24	175
30	14.0 ± 0.27	101 ± 33.9	165 ± 18.5	7	12
33	1.41 ± 0.176	52.7 ± 23.3	>500	37	>350
34	1.05 ± 0.456	43.1 ± 11.0	>500	41	>475
35	26.7 ± 4.97	107 ± 12.7	>500	4	>19

<sup>a</sup> Radioligand binding with [<sup>3</sup>H]-diprenorphine, using membranes from CHO cells expressing human  $\kappa$ ,  $\mu$  or HEK293 cells expressing human  $\delta$  opioid receptors, respectively. Data represent mean ± SEM from at least three independent experiments, unless otherwise noted. <sup>b</sup> Data from one experiment ( $n = 1$ )

**Table 2. In Vitro Inhibition of Agonist-Stimulated [<sup>35</sup>S]GTP- $\gamma$ -S Binding for  $\kappa$ ,  $\mu$ , and  $\delta$  Opioid Receptors**

compd	$\kappa$ $K_b$ (nM) <sup>a</sup>	$\mu$ $K_b$ (nM) <sup>b</sup>	$\delta$ $K_b$ (nM) <sup>c</sup>	$\mu/\kappa$	$\delta/\kappa$
1	0.798 ± 0.146	32.9 ± 5.03	14.1 ± 2.41	41	18
2a	0.0978 ± 0.0178	6.58 ± 0.810	168 ± 16.8	67	1718
2b	0.162 ± 0.0824	11.2 ± 2.46	619 ± 132	69	3821
5	4.33 ± 0.816	3.80 ± 0.491	60.3 ± 6.47	1	14
11	17.0 ± 0.570	150 ± 2.26	635 ± 58.2	9	37
13	5.89 ± 2.06	110 ± 59.2	407 ± 67.0	19	69
18	0.632 ± 0.0805	6.80 ± 0.867	83.3 ± 27.7	11	132
24	3.52 ± 2.30	63.5 ± 8.32	525 ± 113	18	149
25	1.57 ± 0.398	21.3 ± 4.82	293 ± 42.3	14	187
26	88.7 ± 17.9	>500	>1000	>5	>5
29	0.813 ± 0.285	17.4 ± 6.33	110 ± 33.6	21	135
30	44.8 ± 14.7	69.6 ± 22.8	220 ± 149	2	5
34	2.46 ± 0.0809	36.6	338 ± 106	15	137
35	15.2 ± 3.78	43.8	>1000	3	>65

<sup>a</sup> Inhibition of the  $\kappa$  agonist U69,593, using membranes from CHO cells expressing human  $\kappa$  opioid receptors. <sup>b</sup> Inhibition of the  $\mu$  agonist DAMGO, using membranes from CHO cells expressing human  $\mu$  opioid receptors. <sup>c</sup> Inhibition of the  $\delta$  agonist DPDPE, using membranes from HEK293 cells expressing human  $\delta$  opioid receptors.

receptor agonists (U69,593 at  $\kappa$ , DAMGO at  $\mu$ , and DPDPE at  $\delta$ ) can stimulate the binding of the GTP analogue [<sup>35</sup>S]GTP- $\gamma$ -S to G-proteins in membranes. Concentrations of the test compound causing 50% inhibition (IC<sub>50</sub>) of opioid agonist stimulation were determined from 11 point concentration response curves. Results are shown in Table 2.

Compound **25** showed good in vitro antagonist potency and selectivity for  $\kappa$  antagonist functional activity, with  $\kappa$   $K_b = 1.57$  nM,  $\mu$   $K_b = 21.3$  nM, and  $\delta$   $K_b = 293$  nM. Also showing good  $\kappa$  in vitro antagonist potency and selectivity was compound **29**, with  $\kappa$   $K_b = 0.813$  nM,  $\mu$   $K_b = 17.4$  nM, and  $\delta$   $K_b = 110$  nM.

Compounds were also tested for agonist activity in vitro in the GTP- $\gamma$ -S assays for  $\kappa$ ,  $\mu$ , and  $\delta$  opioid receptors. Compounds were tested in a concentration range going up to 10  $\mu$ M. In all cases, compounds were completely devoid of agonist stimulation in the GTP- $\gamma$ -S assay for each of the  $\kappa$ ,  $\mu$ , and  $\delta$  opioid receptors (data not shown). This demonstrates that this series of amino-benzylxyarylamides are consistently pure antagonists for each of the types of opioid receptors.

Compound **25** was evaluated for in vivo  $\kappa$  antagonist activity based on blockade of antinociceptive active of the  $\kappa$  agonist U69,593 in the rat formalin assay.<sup>23</sup> After oral dosing, Compound **25** was a potent antagonist in vivo, with an ED<sub>50</sub> = 0.24 mg/kg for reversal of a 1 mg/kg, sc, dose of U69,593. In contrast, **25** was also evaluated for  $\mu$  antagonist activity in the rat formalin assay based on blockade of morphine. Compound **25** had an ED<sub>50</sub> of 30 mg/kg for reversal of a 10 mg/kg, sc, dose of morphine. This demonstrates that **25** has good in vivo selectivity for antagonism of  $\kappa$  agonist U69,593 compared to  $\mu$  agonist morphine.

Compounds were also evaluated for their potential as receptor occupancy tracers. The only  $\kappa$  receptor occupancy tracer, **4**, previously reported in the literature, is a  $\kappa$  agonist.<sup>16</sup> Finding a receptor occupancy tracer with  $\kappa$  antagonist activity was desired, as this would correspond to the same binding mode for the desired  $\kappa$  antagonist functional activity.

Tracer evaluation was carried out using the LC/tandem mass spectrometry (LC/MS/MS) method of Phebus.<sup>24</sup> Doses of the compounds to be evaluated as potential tracers were selected to be as low as possible while still permitting accurate measurement by LC/MS/MS. Striatal and cerebellar levels of tracer were measured by LC/MS/MS. Striatal levels of tracer represent total binding. Cerebellar levels represent nonspecific binding as this tissue region has little to no expression of  $\kappa$ , nor  $\mu$  or  $\delta$  opioid receptors.<sup>25</sup> Specific binding of the tracer was determined by the method of Wadenberg, calculated by taking the difference in tracer concentration between striatum and cerebellum and then dividing by tracer concentration in cerebellum (e.g., (striatum — cerebellum)/cerebellum). This provides an estimate of  $B_{max}/K_d$ , defined as the binding potential.<sup>26</sup>

Additionally, percent standardized uptake value (%SUV) was calculated as the proportion of the injected tracer dose reaching the target rich tissue—striatum.

$$\%SUV = \frac{[(\text{Tracer Amt Measured in Tissue}) / (\text{Injected Tracer Dose})] \times 100}$$

Data for the antagonists were compared to LC/MS/MS data generated for **4**, given its success as a nonhuman primate  $\kappa$  receptor tracer for positron emission tomography (PET).<sup>16</sup> The results are shown in Table 3. For comparison purposes, also included in Table 3 are calculated values for cLogP, predicted fraction unbound in brain (fu-brain), and predicted 5 min brain to plasma ratio. All of the  $\kappa$  antagonists tested differentially distributed toward the receptor rich striatum relative to cerebellum, except for **2b**. The molecules with superior brain uptake were able to be dosed lower and retain detection by LC/MS/MS. The exception was **13**, which exhibited poor %SUV and further investigation of this compound was halted. Compound **34** exceeded **4** with respect to both binding potential and %SUV.



Table 3. LC/MS/MS Receptor Occupancy Tracer Evaluation

compd	dose iv, (ug/kg)	%SUV <sup>a</sup> (%)	specific to nonspecific binding <sup>b</sup>	cLogP <sup>c</sup>	predicted fu-brain <sup>d</sup>	predicted brain to plasma ratio <sup>d</sup>
2b	3	23	0	5.38	0.007	0.551
4	1.5	50	1.5	4.17	0.053	3.148
13	30	13	2.2	2.62	0.026	0.542
18	3	67	1.2	4.13	0.009	1.622
25	3	2907	0.2	5.23	0.006	3.013
34	1	270	0.3	4.60	0.005	1.982

<sup>a</sup> Standardized uptake value, calculated as  $\%SUV = [(TracerAmtMeasuredinTissue)/(InjectedTracerDose)] \times 100$

<sup>b</sup> Calculated as  $((\text{concentration in striatum}/\text{concentration in cerebellum}) - 1)$ .<sup>26</sup> <sup>c</sup> cLogP method calculated from BioByte. <sup>d</sup> See Experimental Section for computational chemistry methods.

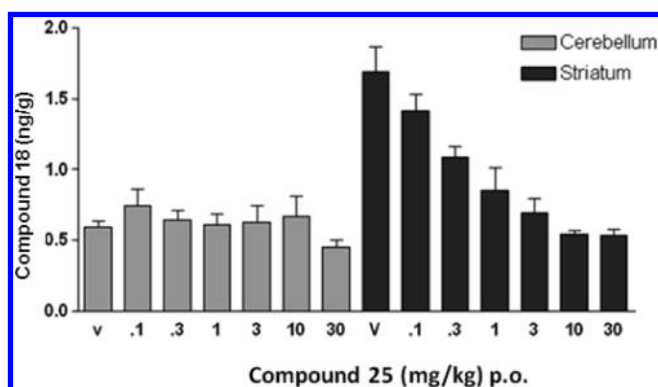


Figure 2. Brain concentrations of compound 18, 40 min post dosing (3 ug/kg, iv), pretreated (1 h) with compound 25, at the doses listed.

Compound 18 was comparable to 4 regarding both its %SUV and binding potential. All tracer candidates displayed appropriate kinetics such that both brain uptake and washout would occur in a short time frame. In all cases peak uptake and washout have occurred by 40 min following iv tracer dosing.

Blockade of tracer doses of compound 18 was demonstrated by pretreatment with compound 25, as shown in Figure 2. Increasing doses of 25 can be seen to reduce brain concentrations of tracer compound 18 in a dose-dependent manner in both striatum and thalamus,  $\kappa$  receptor rich brain regions.<sup>27</sup> In contrast, no effect is seen in cerebellum, which has low expression of  $\kappa$  receptors. These data illustrate that cerebellum serves as a useful null region and that the relative ratio of tracer levels of compound 18 striatum compared to cerebellum provides a practical method for determining receptor occupancy levels of  $\kappa$  opioid receptors.

The utility of compound 18 as a tracer for receptor occupancy determination was demonstrated in displacement experiments. Receptor occupancy of compound 25 was determined using 3 ug/kg, iv, tracer doses of compound 18. After oral doses, ranging from 0.1 to 30 mg/kg, it was determined that compound 25 had an  $ED_{50} = 0.06$  mg/kg for occupancy of  $\kappa$  opioid receptors, as shown in Figure 3.

## DISCUSSION

We have previously reported aminobenzoyloxyarylamides with potent opioid antagonist activity.<sup>17</sup> These previous compounds showed little to no selectivity between  $\kappa$ ,  $\mu$ , and  $\delta$  opioid receptor activity. Compound 5, with a benzyl amine substituent, showed an opioid receptor selectivity profile with highest and nearly

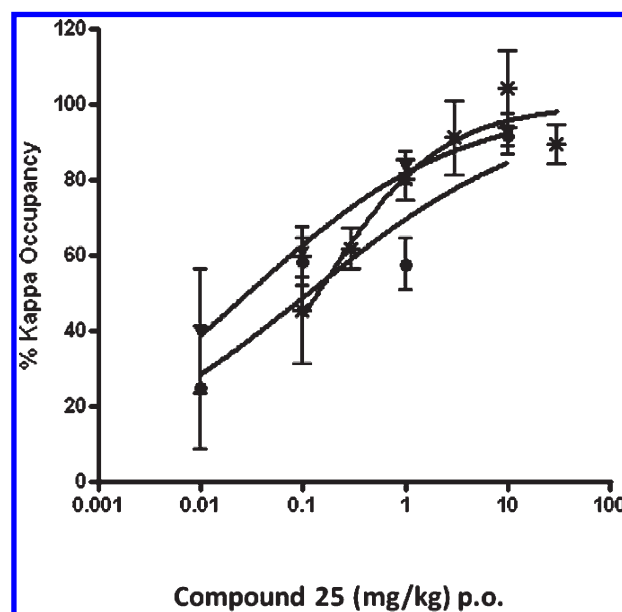


Figure 3. Compound 25 dose-dependently occupies  $\kappa$  opioid receptors in rat striatum, as assessed by antagonist tracer 18. Tracer 18 was given intravenously at 3  $\mu$ g/kg with a 40 min survival interval.

equal affinity for  $\kappa$  and  $\mu$  receptors, with about 10-fold weaker affinity for  $\delta$  receptors. Introduction of ring constraint, as with the pyrrolidine in compound 10, somewhat increased selectivity in favor of  $\kappa$  receptor activity. Additional compounds were prepared to examine the affect on both  $\kappa$  receptor affinity and selectivity that resulted from changes in either the aryl substituent on the pyrrolidine ring or in the aryl amide ring.

Replacing the phenyl group on the pyrrolidine with a pyridine, as in compound 13, gave good  $\kappa$  receptor affinity and selectivity. Changing the nicotinamide group to a halogen substituted benzamide, combined with the pyridinyl pyrrolidine, gave greatly improved  $\kappa$  receptor affinity and selectivity, as exemplified by chlorobenzamide 17. Pyrrolidine substitution with a 3-fluorophenyl group combined with fluorobenzamide functionality, as in 24, also gave good  $\kappa$  receptor affinity and selectivity. Variation in ring constraint was also examined by changing the pyrrolidine to azetidine functionality, as in compound 33. This compound showed good  $\kappa$  receptor affinity and selectivity, as well.

The racemic compounds were resolved into individual enantiomers by chiral chromatography. For each of the arylpyrrolidines, the best  $\kappa$  receptor affinity was found for the (S)-enantiomer.

The (S)-enantiomers also consistently showed even better  $\kappa$  receptor selectivity than their corresponding racemates. This is exemplified by a comparison of the enantiomeric pair of compounds **25** and **26**, showing an enantiomeric potency ratio of 95 based on their respective  $\kappa$  receptor affinities. Similarly, the enantiomeric pair of **18** and **19** show an enantiomeric potency ratio of 62 based on affinity for  $\kappa$  receptors.

Evaluation of the compounds for in vitro functional antagonist activity in a GTP- $\gamma$ -S binding assay showed antagonist potency that was in good agreement with the affinities found in the receptor binding assay. The observed selectivity profiles were also concordant between receptor binding affinity and functional antagonist potency. All of the compounds were also found to be pure antagonists, completely devoid of agonist activity when tested in the GTP- $\gamma$ -S functional assay for  $\kappa$  as well as  $\mu$  and  $\delta$  activities.

These compounds show good central activity after oral dosing, as demonstrated by blockade of the antinociceptive activity of the  $\kappa$  agonist U69,593 in the formalin assay in rat, with compound **25** having an  $AD_{50}$  = 0.24 mg/kg, po. The practical utility of compound **25** as a selective  $\kappa$  antagonist for in vivo experiments was further demonstrated by the lack of activity for antagonism of morphine antinociception in the formalin assay in rat, even with antagonist doses of compound **25** as high as 30 mg/kg, po. These compounds show potent in vivo antagonist activity within 30 min of oral dosing, which is in marked contrast to the delayed onset of activity reported for some  $\kappa$  antagonists such as **2a** and **1**.<sup>28</sup>

Compounds from this series were also found to have suitable properties for development as receptor occupancy tracers. The application of LC/MS/MS technology to tracer discovery enables high-throughput in vivo analyses of potential tracers through terminal rodent experiments. Such experiments provide data to determine if a potential structure is worth labeling and scanning in nonhuman primate, both costly processes.

Prior to this, the only successful  $\kappa$  receptor occupancy tracer has been the agonist compound **4**. It was desired to find a receptor occupancy tracer based on an antagonist scaffold. Because of potential differences in binding interactions between the receptor and agonist versus antagonist compounds, having an antagonist tracer would be most suitable for investigating receptor occupancy of antagonist compounds.

Receptor occupancy tracer evaluation was carried out based on LC/MS/MS detection of brain concentrations of the compounds being tested. Results for predicted properties from computational models that may be relevant for receptor occupancy tracer performance are shown in Table 3. Values for cLogP are often used in the literature for evaluating potential tracer properties of compounds.<sup>29</sup> With the present data set, cLogP values were not predictive of either measured brain uptake (%SUV) or measured binding potential (BP) values. Predicted 5 min brain-to-plasma ratios afforded a better computational tool for assessing potential for good brain uptake. The low 5 min brain-to-plasma ratios for compounds **13** and for **2b** matches the low %SUV values for both of these compounds. Predicted unbound fraction in brain (fu-brain) values were indicative of measured binding potential results for most of the compounds in the data set. Many of the compounds with predicted fu-brain  $\geq 0.009$  in turn had good measured BP results, as exemplified by compounds **4**, **13**, and **18**. Correspondingly, the low predicted fu-brain for **2b** matched its very low measured binding potential.

Compound **18** showed good differential distribution between striatal versus cerebellum, as indicated by a ratio of brain levels of **18** that were about 2-fold higher in striatum than cerebellum, an

indication of the level of nonspecific binding needed for good receptor occupancy tracer performance. This was quantified by calculation of a binding potential of 1.2 for compound **18** based on this differential distribution between the  $\kappa$  receptor rich striatum compared to the low  $\kappa$  receptor expression in cerebellum. Good uptake into brain was also found with **18**, which showed a percent standard uptake value (%SUV) of 67% based on brain concentrations in striatum. Potential utility of compound **18** as a  $\kappa$  receptor occupancy tracer was demonstrated by the dose-dependent blockade of tracer doses of **18**, after pretreatment with compound **25**, as shown in Figure 2. The suitability of using **16** for the preclinical determination of  $\kappa$  opioid receptor occupancy levels in rat by the LC/MS/MS method was illustrated in Figure 3, showing that compound **25** had potent occupancy of  $\kappa$  opioid receptors, with an  $ED_{50}$  = 0.06 mg/kg after oral administration. Further development of **25** as a PET tracer will be reported in due course.

## CONCLUSIONS

Highly potent and selective antagonists for  $\kappa$  opioid receptors have been found in compounds from the aminobenzyloxyarylamide scaffold. Incorporating ring constraint with an arylpyrrolidine substitution resulted in high affinity and selectivity for  $\kappa$  opioid receptors. Compound **25** showed good affinity and selectivity for  $\kappa$  opioid receptors in vitro and was also a pure antagonist in GTP- $\gamma$ -S functional assays. Compound **25** also showed good in vivo potency and selectivity after oral dosing. It reversed the antinociceptive activity of the  $\kappa$  agonist U69,593 in the rat formalin assay, with an  $AD_{50}$  = 0.24 mg/kg, po. In contrast, it did not block the activity of the  $\mu$  agonist morphine in the rat formalin assay, even at doses up to 30 mg/kg, po. This demonstrates a broad selectivity window for selectively investigating the effects of  $\kappa$  opioid antagonists in the rat. Compound **29** also showed good affinity and selectivity for  $\kappa$  receptors and may be also be of interest for further investigation.

Compounds from this series were also evaluated for potential use as receptor occupancy tracers for  $\kappa$  opioid receptors. The only tracer reported to date for  $\kappa$  opioid receptors is **4**, which is an agonist for  $\kappa$  opioid receptors. It was desired to find a potential tracer from this new series that would have  $\kappa$  antagonist properties, as this would presumably interact at the receptor in the same binding mode and be more suitable for evaluating receptor occupancy of other  $\kappa$  antagonist compounds. This work illustrates the usefulness of the LC/MS/MS method for the evaluation of unlabeled compounds for potential use as receptor occupancy tracers. Compounds could be evaluated more rapidly and more economically because radiolabeling is not necessary due to the use of mass spectrometry for detection of test compounds. The results reported here demonstrate that the LC/MS/MS data are able to rapidly compare diverse compounds on three key properties predicting PET tracer performance: (1) specific to nonspecific binding (e.g., binding potential), (2) %SUV, and (3) kinetics.

Compound **18** showed good in vivo tracer properties when benchmarked in comparison with the agonist tracer, **4**. This compound showed good binding potential and good brain uptake, as shown in Table 3. It was also demonstrated that tracer doses of compound **18** could be blocked by pretreatment with compound **25** in a dose-dependent manner. This demonstrates the suitability of using compound **18** as a tracer for determining  $\kappa$  opioid receptor occupancy levels of other compounds.

## ■ EXPERIMENTAL SECTION

**Chemistry. General Methods.** All reagents and anhydrous solvents were obtained from commercial sources and used without further purification unless noted otherwise.  $^1\text{H}$  and  $^{13}\text{C}$  NMR spectra were recorded on a Varian 300 or 400 MHz spectrometer (as indicated). Chemical shifts are reported in ppm with the solvent resonance as the internal standard ( $\text{CDCl}_3$  7.26 ppm, 77.00 ppm, methanol- $d_4$  3.31 ppm, 49.1 ppm,  $\text{DMSO}-d_6$  2.49 ppm, 39.51 ppm for  $^1\text{H}$ ,  $^{13}\text{C}$ , respectively).

Optical rotations were measured with a 341 polarimeter (Perkin-Elmer) at 20 °C and at 589 nm (sodium lamp).

Vibrational circular dichroism (VCD): samples were dissolved in  $\text{CDCl}_3$  to achieve a final concentration of approximately 20 mg/mL. The VCD and IR spectra were obtained with a resolution of  $4\text{ cm}^{-1}$  using ChiralIR FT VCD spectrometer (BioTools Inc.) with an IR cell equipped with  $\text{BaF}_2$  windows and a path length of 100 mm. The VCD and IR were collected for 4 h with 150 mL of the sample. A spectrum of the neat solvent obtained under similar conditions was used to identify background signals and instrument drift. Vibrational frequencies and absorption and VCD intensities were obtained by optimizing the lowest energy conformers (generated by Monte Carlo conformational search and clustering using Maestro 8.0) with Gaussian at the B3PW91/6-31G\*\* level of theory, and the corresponding spectra were simulated using a Lorentzian bandwidth of  $6\text{ cm}^{-1}$ . Assignment of configuration was made based on comparison of theoretical calculated spectra with experimentally measured spectra.

Compounds were analyzed for purity by HPLC and HPLC-MS and purities of synthesized compounds were all found to be  $\geq 95\%$  by the methods 1 and 2, as specified below.

**HPLC Method 1.** Hitachi L7000 HPLC, Zorbax SB-Phenyl C18 column  $4.6\text{ mm} \times 150\text{ mm} \times 5\text{ }\mu\text{m}$ , 5% acetonitrile/95% (0.1% trifluoroacetic acid in water) held for 1 min, 3 min gradient with a 4 min hold to 95% acetonitrile/5% (0.1% trifluoroacetic acid in water). Flow rate 1.0 mL/min,  $\lambda = 254\text{ nm}$ .

**HPLC-MS Method 2.** Agilent 1000 HPLC, Phenomenex Gemini C18  $2.0\text{ mm} \times 50\text{ mm} \times 3.0\text{ }\mu\text{m}$ , 5–100% ACN in water (both containing 0.1% formic acid), 7.0 min gradient with a 1 min hold. Flow rate 1.0 mL/min. Atmospheric pressure ionization-electrospray (API-ES) mass spectra data were acquired with an Agilent Technologies MSD single quadrupole coupled to an HP1100 LC system.

**ES-MS Method 3.** Mass spectra were recorded on a Waters 2790 HPLC coupled to a Waters ZMD with an electrospray ionization source. Eluent was 80% methanol and 20% water containing 6.5 nM ammonium acetate at 1 mL/min for 0.5 min.

**Chiral HPLC Method 4.** HPLC, Chiralpak AS-H  $4.6\text{ mm} \times 150\text{ mm}$ , 0.2% *N,N*-dimethylethylamine in methanol. Flow rate 1.0 mL/min.  $\lambda = 225\text{ nm}$ .

**Chiral HPLC Method 5.** Shimadzu HPLC, Chiralpak AD  $4.6\text{ mm} \times 150\text{ mm}$ , 0.2% *N,N*-dimethylethylamine in ethanol. Flow rate 0.6 mL/min.  $\lambda = 249\text{ nm}$ .

**Chiral HPLC Method 6.** HPLC, Chiralpak AD  $4.6\text{ mm} \times 150\text{ mm}$ , 0.2% *N,N*-dimethylethylamine in ethanol. Flow rate 0.75 mL/min.  $\lambda = 225\text{ nm}$ .

**Chiral HPLC Method 7.** HPLC, Chiralpak AD-H  $4.6\text{ mm} \times 150\text{ mm}$ , 0.2% *N,N*-dimethylethylamine in 80% heptanes, 10% ethanol, 10% methanol. Flow rate 0.6 mL/min.  $\lambda = 270\text{ nm}$ .

**Chiral HPLC Method 8.** HPLC, Chiralcel OJ-H,  $4.6\text{ mm} \times 150\text{ mm}$ , 0.2% *N,N*-dimethylethylamine in 70% methanol, 30% acetonitrile. Flow rate 0.6 mL/min.  $\lambda = 250\text{ nm}$ .

**SNAr. General Procedure A.** As an example, potassium carbonate (2 equiv, 400 mmol) was added to a solution of 4-hydroxybenzaldehyde (1 equiv), 4-halobenzonitrile (1 equiv, 200 mmol), and dimethylacetamide (0.4M, 475 mL). The reaction was heated to 100 °C for 2 h. The reaction was cooled to room temperature and then poured into 1.4 L of

ice water. The resulting tan solid was collected by filtration, washed with water ( $2 \times 150\text{ mL}$ ), and then dried in a vacuum oven to afford the 4-(4-formylphenoxy)benzonitrile.

**Nitrile Oxidation. General Procedure B.** As an example, potassium carbonate (0.5 equiv, 96 mmol) was added to a solution of 4-(4-formylphenoxy)benzonitrile (1 equiv, 192 mmol), and DMSO (1.1M, 170 mL), cooled to 10 °C, and then 30%  $\text{H}_2\text{O}_2(\text{aq})$  (1.1 equiv, 211 mmol) was added dropwise to the reaction. The reaction was allowed to warm to room temperature and then stirred for 2 h and then poured into ice water and then collected the tan precipitate via filtration with a Büchner funnel. The precipitate was washed with water ( $3 \times 100\text{ mL}$ ) and then dried in a vacuum oven at 50 °C to yield 4-(4-formylphenoxy)-benzamide.

**Reductive Amination. General Procedure C.** As an example, to a solution amine (1.2 equiv, 3.4 mmol), 4-(4-formylphenoxy)benzamide (1 equiv, 2.8 mmol), and 1,2-dichloroethane (0.2M, 15 mL) was added powdered 3 Å molecular sieves. The mixture was stirred at room temperature overnight, whereupon sodium triacetoxyborohydride (2.5 equiv, 7.0 mmol) and acetic acid (2.5 equiv, 7.0 mmol) were added to the reaction. After stirring at room temperature for 3 h, the reaction was filtered through Celite, quenched with saturated aqueous sodium bicarbonate (20 mL), and then extracted with ethyl acetate ( $3 \times 25\text{ mL}$ ). The combined organic extracts were dried over magnesium sulfate, filtered, and then concentrated on a rotary evaporator. The resulting crude material was purified by flash chromatography on silica gel eluting with 1–25% (10% ammonium hydroxide (aq) in ethanol) in 1:1 dichloromethane:hexanes to afford 4-[4-(aminomethyl)phenoxy]benzamide.

**Enantiomeric Separation by Chiral Chromatography. General Procedure D.** Isomers of racemic material were isolated by preparative HPLC utilizing a Chiralpak AD column ( $8\text{ cm} \times 29\text{ cm}$ ) eluting with 0.2% DMEA in ethanol at a rate 350 mL/min.

**Enantiomeric Separation by Chiral Chromatography. General Procedure E.** Isomers of racemic material were isolated by preparative HPLC utilizing a Chiralpak AS-H column ( $3\text{ cm} \times 25\text{ cm}$ ) eluting with 0.2% DMEA in methanol at a rate of 30 mL/min.

**Enantiomeric Separation by Chiral Chromatography. General Procedure F.** Isomers of racemic material were isolated by preparative HPLC utilizing a Chiralpak AD column ( $8\text{ cm} \times 32\text{ cm}$ ) eluting with 80% heptanes, 10% ethanol, 10% methanol each containing 0.2% DMEA in at a rate of 350 mL/min.

**6-(4-Formylphenoxy)pyridine-3-carbonitrile (8).** Compound 8 was prepared from 4-hydroxybenzaldehyde and 6-fluoropyridine-3-carbonitrile using general procedure A. Yield (96%).  $^1\text{H}$  NMR (300 MHz, DMSO): 10.03 (s, 1H), 8.70 (d,  $J = 2.3\text{ Hz}$ , 1H), 8.41 (dd,  $J = 2.3, 8.6\text{ Hz}$ , 1H), 8.05–8.00 (m, 2H), 7.48–7.44 (m, 2H), 7.40–7.37 (m, 1H).

**6-(4-Formylphenoxy)pyridine-3-carboxamide (9).** Compound 9 was prepared from 8 using general procedure B. Yield (79%).  $^1\text{H}$  NMR (300 MHz, DMSO): 10.02 (s, 1H), 8.67 (d,  $J = 2.0\text{ Hz}$ , 1H), 8.34 (dd,  $J = 2.3, 8.6\text{ Hz}$ , 1H), 8.13–8.06 (m, 1H), 8.03–7.98 (m, 2H), 7.55 (s, 1H), 7.42–7.38 (m, 2H), 7.24 (d,  $J = 8.6\text{ Hz}$ , 1H).

**6-[4-[(2-Phenylpyrrolidin-1-yl)methyl]phenoxy]pyridine-3-carboxamide (11).** Compound 11 was prepared from 9 using general procedure C. Yield (70%). HPLC = 99% at 5.9 min by HPLC method 1, mass spectrum ( $m/z$ ): 374.25 ( $M + 1$ ) by ES-MS method 3.  $^1\text{H}$  NMR (300 MHz,  $\text{CDCl}_3$ ): 8.62 (d,  $J = 2.0\text{ Hz}$ , 1H), 8.19 (dd,  $J = 2.3, 8.6\text{ Hz}$ , 1H), 7.50 (d,  $J = 7.3\text{ Hz}$ , 2H), 7.40–7.36 (m, 4H), 7.31–7.26 (m, 1H), 7.09 (d,  $J = 8.6\text{ Hz}$ , 2H), 6.96 (d,  $J = 8.6\text{ Hz}$ , 1H), 6.09–5.96 (m, 2H), 3.88 (d,  $J = 13.2\text{ Hz}$ , 1H), 3.45–3.40 (m, 1H), 3.22–3.09 (m, 2H), 2.30–2.18 (m, 2H), 1.98–1.84 (m, 3H).

**6-[4-[[2-(3-Pyridyl)pyrrolidin-1-yl]methyl]phenoxy]pyridine-3-carboxamide (13).** Compound 13 was prepared from 9 using general procedure C. Yield (33%). HPLC = 100% at 5.54 min by HPLC method 1, mass spectrum ( $m/z$ ): 375.22 ( $M + 1$ ) by ES-MS method 3.  $^1\text{H}$  NMR (400.15 MHz, DMSO): 8.63 (m, 2H), 8.49 (dd,  $J = 1.8, 4.8\text{ Hz}$ ,



1H), 8.26 (dd,  $J = 2.4, 8.6$  Hz, 1H), 8.04 (s, 1H), 7.87 (dt,  $J = 7.9, 2.0$  Hz, 1H), 7.48 (s, 1H), 7.42–7.39 (m, 1H), 7.31 (d,  $J = 8.3$  Hz, 2H), 7.10–7.04 (m, 3H), 3.67 (d,  $J = 13.2$  Hz, 1H), 3.51 (t,  $J = 8.1$  Hz, 1H), 3.20 (d,  $J = 13.2$  Hz, 1H), 3.09–3.04 (m, 1H), 2.31–2.21 (m, 2H), 1.91–1.84 (m, 2H), 1.69–1.64 (m, 1H).

**3-Chloro-4-(4-formylphenoxy)benzonitrile (15).** Compound **15** was prepared from 4-hydroxybenzaldehyde and 3-chloro-4-fluorobenzonitrile using general procedure A. Yield (84%).  $^1\text{H}$  NMR (300 MHz, DMSO): 9.97 (s, 1H), 8.31 (d,  $J = 1.8$  Hz, 1H), 8.00–7.89 (m, 3H), 7.39–7.35 (m, 1H), 7.26–7.23 (m, 2H).

**3-Chloro-4-(4-formylphenoxy)benzamide (16).** Compound **16** was prepared from **15** using general procedure B. Yield (97%).  $^1\text{H}$  NMR (300 MHz, DMSO): 9.95 (s, 1H), 8.14 (m, 2H), 7.97–7.91 (m, 3H), 7.58 (bs, 1H), 7.36 (d,  $J = 8.7$  Hz, 1H), 7.18–7.13 (m, 2H).

**3-Chloro-4-[4-[[2-(3-pyridyl)pyrrolidin-1-yl]methyl]phenoxy]benzamide (17).** Compound **17** was prepared from **16** using general procedure C. Yield (73%). HPLC = 100% at 1.44 min, mass spectrum ( $m/z$ ): 408.2 ( $M + 1$ ) by HPLC-MS method 2.  $^1\text{H}$  NMR (300 MHz, DMSO): 8.59 (d,  $J = 1.3$  Hz, 1H), 8.47 (dd,  $J = 1.3, 4.9$  Hz, 1H), 8.08 (d,  $J = 1.8$  Hz, 1H), 8.04 (bs, 1H), 7.85–7.80 (m, 2H), 7.46 (bs, 1H), 7.37 (dd,  $J = 4.3, 7.3$  Hz, 1H), 7.29 (d,  $J = 8.5$  Hz, 2H), 7.00–6.93 (m, 3H), 3.62 (d,  $J = 12.8$  Hz, 1H), 3.49 (t,  $J = 8.5$  Hz, 1H), 3.21 (d,  $J = 12.8$  Hz, 1H), 3.04 (m, 1H), 2.31–2.16 (m, 2H), 1.91–1.73 (m, 2H), 1.68–1.55 (m, 1H).

**3-[(2R)-Pyrrolidin-2-yl]pyridine and 3-[(2S)-Pyrrolidin-2-yl]pyridine.** Enantiomers of racemic 3-pyrrolidin-2-ylpyridine (0.5 g, 3.4 mmol) were separated by supercritical fluid chromatography (SFC) utilizing a Berger Multigram Supercritical Fluid chromatograph with a Chiralpak AD-H column (2.1 cm  $\times$  25 cm  $\times$  5  $\mu\text{m}$ ). The components were eluted with 15% methanol (containing 0.2% DMEA) in  $\text{CO}_2$  at 70 mL/min monitoring at  $\lambda = 225$  nm. Fractions containing each separated isomer were combined and evaporated to yield isomer 1, compound X2, and isomer 2, compound X3. Optical purity was determined by chiral supercritical fluid chromatography on a Berger Minigram Supercritical Fluid chromatograph with a Chiralpak AD-H column (4.6 mm  $\times$  150 mm  $\times$  5  $\mu\text{m}$ ). The components were eluted with 10% methanol (containing 0.2% DMEA) in  $\text{CO}_2$  at 5 mL/min monitoring at  $\lambda = 230$  nm. Absolute configuration of the separated enantiomers of 3-pyrrolidin-2-ylpyridine were determined by specific rotation as reported in ref 20. **3-[(2R)-pyrrolidin-2-yl]pyridine:** Yield = 25%. Chiral HPLC = 100% at 2.18 min. Specific rotation =  $[\alpha]_{\text{D}}^{23} +36.30$  ( $c$  1.00, MeOH). **3-[(2S)-pyrrolidin-2-yl]pyridine:** Yield = 30%. Chiral HPLC = 99% at 2.62 min. Specific rotation =  $[\alpha]_{\text{D}}^{23} -36.20$  ( $c$  1.00, MeOH).

**3-Chloro-4-[4-[(2S)-2-(3-pyridyl)pyrrolidin-1-yl]methyl]phenoxy]benzamide (18).** Compound **18** was prepared from **17** using general procedure E. Yield (40%). HPLC = 100% at 1.41 min, mass spectrum ( $m/z$ ): 408.2 ( $M + 1$ ) by HPLC-MS method 2. Chiral HPLC = 99% at 3.612 min by chiral HPLC method 4, Specific rotation =  $[\alpha]_{\text{D}}^{20} +30.21$  ( $c$  1.00, EtOH).  $^1\text{H}$  NMR (399.83 MHz, DMSO): 8.55 (d,  $J = 1.3$  Hz, 1H), 8.43 (dd,  $J = 1.5, 4.6$  Hz, 1H), 8.05 (d,  $J = 2.2$  Hz, 1H), 8.00 (s, 1H), 7.81–7.78 (m, 2H), 7.45–7.42 (m, 1H), 7.34 (dd,  $J = 4.8, 7.9$  Hz, 1H), 7.26–7.24 (m, 2H), 6.95–6.91 (m, 3H), 3.59 (d,  $J = 13.2$  Hz, 1H), 3.45 (t,  $J = 8.1$  Hz, 1H), 3.29 (m, 1H), 3.17 (d,  $J = 13.2$  Hz, 1H), 3.03–2.98 (m, 1H), 2.27–2.17 (m, 2H), 1.88–1.55 (m, 2H).

**3-Chloro-4-[4-[(2S)-2-(3-pyridyl)pyrrolidin-1-yl]methyl]phenoxy]benzamide (18).** To a solution 3-[(2S)-pyrrolidin-2-yl]pyridine (1.0 equiv, 0.54 mmol), 3-chloro-4-(4-formylphenoxy)benzamide (1 equiv, 0.54 mmol), and 1,2-dichloroethane (0.02M, 27 mL) was added sodium triacetoxyborohydride (1.5 equiv, 0.82 mmol) and acetic acid (1.5 equiv, 0.82 mmol) were added to the reaction. After stirring at room temperature overnight, the reaction was quenched with saturated aqueous sodium bicarbonate (20 mL) and then extracted with ethyl acetate (3  $\times$  100 mL). The combined organic extracts were dried over magnesium sulfate, filtered, and then concentrated on a rotary evaporator. The resulting crude material was purified by flash chromatography on silica

gel eluting with 2–20% (10% ammonium hydroxide (aq) in ethanol) in 1:1 dichloromethane:hexanes to afford 3-chloro-4-[4-[(2S)-2-(3-pyridyl)pyrrolidin-1-yl]methyl]phenoxy]benzamide. Yield (68%). HPLC = 100% at 1.39 min by HPLC method 2, mass spectrum ( $m/z$ ): 408.2 ( $M + 1$ ). Chiral HPLC = 99% at 3.69 min by chiral HPLC method 4. The retention time of this compound matches the retention time of the first eluting peak from enantiomers previously separated by preparative chiral HPLC.  $^1\text{H}$  NMR (399.83 MHz, DMSO): 8.55 (s, 1H), 8.44–8.43 (m, 1H), 8.05 (s, 1H), 8.01 (s, 1H), 7.79 (d,  $J = 8.4$  Hz, 2H), 7.42 (s, 1H), 7.33 (t,  $J = 5.9$  Hz, 1H), 7.25 (d,  $J = 7.0$  Hz, 2H), 6.94–6.91 (m, 3H), 3.60–3.57 (m, 1H), 3.45 (t,  $J = 8.1$  Hz, 1H), 3.29 (s, 1H), 3.17 (d,  $J = 13.2$  Hz, 1H), 3.00 (t,  $J = 8.1$  Hz, 1H), 2.26–2.15 (m, 2H), 1.88–1.55 (m, 2H).

**3-Chloro-4-[4-[(2R)-2-(3-pyridyl)pyrrolidin-1-yl]methyl]phenoxy]benzamide (19).** Compound **19** was prepared from **17** using general procedure E. Yield (38%). HPLC = 100% at 1.42 min, mass spectrum ( $m/z$ ): 408.2 ( $M + 1$ ) by HPLC-MS method 2. Chiral HPLC = 100% at 5.246 min by chiral HPLC method 4. Specific rotation =  $[\alpha]_{\text{D}}^{20} -23.87$  ( $c$  1.00, EtOH).  $^1\text{H}$  NMR (399.83 MHz, DMSO): 8.55 (d,  $J = 1.8$  Hz, 1H), 8.43 (dd,  $J = 1.5, 4.6$  Hz, 1H), 8.05 (d,  $J = 2.2$  Hz, 1H), 8.03–8.01 (m, 1H), 7.79 (dd,  $J = 2.0, 8.6$  Hz, 2H), 7.42 (s, 1H), 7.34 (dd,  $J = 4.6, 7.7$  Hz, 1H), 7.25 (d,  $J = 8.4$  Hz, 2H), 6.93 (dd,  $J = 5.9, 8.6$  Hz, 3H), 3.59 (d,  $J = 13.2$  Hz, 1H), 3.45 (t,  $J = 8.1$  Hz, 1H), 3.29 (m, 1H), 3.17 (d,  $J = 13.2$  Hz, 1H), 3.03–2.98 (m, 1H), 2.27–2.15 (m, 2H), 1.87–1.55 (m, 2H).

**3-Chloro-4-[4-[(2R)-2-(3-pyridyl)pyrrolidin-1-yl]methyl]phenoxy]benzamide (19).** Compound **19** was prepared from 3-[(2R)-pyrrolidin-2-yl]pyridine using procedure for the preparation of **18**. Yield (59%). HPLC = 100% at 1.38 min by HPLC method 2, mass spectrum ( $m/z$ ): 408.2 ( $M + 1$ ). Chiral HPLC = 100% at 5.44 min by chiral HPLC method 4. The retention time of this compound matches the retention time of the second eluting peak from enantiomers previously separated by preparative chiral HPLC.  $^1\text{H}$  NMR (399.83 MHz, DMSO): 8.55 (s, 1H), 8.44–8.43 (m, 1H), 8.29–8.25 (m, 0H), 8.03 (d,  $J = 17.6$  Hz, 2H), 7.79 (d,  $J = 8.4$  Hz, 2H), 7.42–7.39 (m, 1H), 7.33 (t,  $J = 5.7$  Hz, 1H), 7.25 (d,  $J = 7.0$  Hz, 2H), 6.94–6.91 (m, 3H), 3.60–3.57 (m, 1H), 3.45 (t,  $J = 8.1$  Hz, 1H), 3.28 (s, 1H), 3.17 (d,  $J = 13.2$  Hz, 1H), 3.02–2.98 (m, 1H), 2.26–2.15 (m, 2H), 1.88–1.55 (m, 2H).

**3-Fluoro-4-(4-formylphenoxy)benzonitrile (21).** Compound **21** was prepared from 4-hydroxybenzaldehyde and 3, 4-difluorobenzonitrile using general procedure A. Yield (72%).  $^1\text{H}$  NMR (300 MHz, DMSO): 9.92 (s, 1H), 7.98–7.89 (m, 2H), 7.76 (dd,  $J = 1.8, 10.3$  Hz, 1H), 7.65–7.56 (m, 1H), 7.34 (d,  $J = 8.1$  Hz, 1H), 7.22–7.12 (m, 2H).

**3-Fluoro-4-(4-formylphenoxy)benzamide (22).** Compound **22** was prepared from **21** using general procedure B. Yield (100%). HPLC = 100% at 3.19 min by HPLC method 2, mass spectrum ( $m/z$ ): 260 ( $M + 1$ ).  $^1\text{H}$  NMR (300 MHz, DMSO): 9.94 (s, 1H), 8.11 (bs, 1H), 7.98–7.88 (m, 3H), 7.74–7.78 (m, 1H), 7.58 (bs, 1H), 7.41 (t,  $J = 8.2$  Hz, 1H), 7.22–7.15 (m, 2H).

**3-Fluoro-4-[4-[[2-(3-fluorophenyl)pyrrolidin-1-yl]methyl]phenoxy]benzamide (24).** Compound **24** was prepared from **21** and 2-(3-fluorophenyl)pyrrolidine using general procedure C. Yield (27%). HPLC = 98% at 4.161 min by HPLC-MS method 2, mass spectrum ( $m/z$ ): 409 ( $M + 1$ ).  $^1\text{H}$  NMR (300 MHz, MeOD): 7.77 (dd,  $J = 2.6, 11.7$  Hz, 1H), 7.66 (m, 1H), 7.40–7.16 (m, 5H), 7.03–6.93 (m, 4H), 3.74 (d,  $J = 12.8$  Hz, 1H), 3.42 (t,  $J = 8.0$  Hz, 1H), 3.16 (t,  $J = 12.8$  Hz, 1H), 3.10 (m, 1H), 2.35–2.16 (m, 2H), 1.97–1.62 (m, 3H).

**3-Fluoro-4-[4-[(2S)-2-(3-fluorophenyl)pyrrolidin-1-yl]methyl]phenoxy]benzamide (25).** Compound **25** was prepared from **24** using general procedure D. Compound **25** was obtained after chiral chromatography utilizing a Chiralpak AD (20 mm  $\times$  250 mm  $\times$  10  $\mu\text{m}$ ) eluting with 0.2% DMEA in ethanol at 8 mL/min monitoring at  $\lambda = 254/325$  nm. Yield (42%). HPLC = 100% at 4.17 min by HPLC-MS method 2, mass spectrum ( $m/z$ ): 409 ( $M + 1$ ). Chiral HPLC = 98% at 5.772 min by chiral HPLC method 6. Specific rotation =  $[\alpha]_{\text{D}}^{20} -23.26$  ( $c$  1.00,

EtOH).  $^1\text{H}$  NMR (300 MHz, MeOD): 7.76 (dd,  $J = 2.2$ , 11.7 Hz, 1H), 7.66 (m, 1H), 7.39–7.15 (m, 5H), 7.04–6.91 (m, 4H), 3.74 (d,  $J = 12.8$  Hz, 1H), 3.42 (t,  $J = 8.0$  Hz, 1H), 3.16 (d, 1H,  $J = 12.8$  Hz, 1H), 3.15–3.05 (m, 1H), 2.35–2.15 (m, 2H), 1.98–1.61 (m, 3H).

**3-Fluoro-4-[4-[(2R)-2-(3-fluorophenyl)pyrrolidin-1-yl]methyl]phenoxy]benzamide (26).** Compound **26** was prepared from **24** using general procedure D. Compound **26** was obtained after chiral chromatography utilizing a Chiralpak AD (20 mm  $\times$  250 mm  $\times$  10  $\mu\text{m}$ ) eluting with 0.2% DMEA in ethanol at 8 mL/min monitoring at  $\lambda = 254/325$  nm. Yield (42%). HPLC = 100% @ 4.15 min by HPLC-MS method 2, mass spectrum ( $m/z$ ): 409 ( $M + 1$ ). Chiral HPLC = 98% at 7.221 min by chiral HPLC method 6. Specific rotation =  $[\alpha]_{\text{D}}^{20} +23.87$  ( $c$  1.00, EtOH).  $^1\text{H}$  NMR (300 MHz, MeOD): 7.76 (dd,  $J = 2.6$ , 11.7 Hz, 1H), 7.66 (m, 1H), 7.38–7.17 (m, 5H), 7.04–6.91 (m, 4H), 3.74 (d, 1H,  $J = 12.8$  Hz, 1H), 3.42 (d,  $J = 8.2$  Hz, 1H), 3.16 (d,  $J = 12.8$  Hz, 1H), 3.15–3.04 (m, 1H), 2.36–2.16 (m, 2H), 1.99–1.60 (m, 3H).

**3-Fluoro-4-[4-[(2R)-2-(3-fluorophenyl)pyrrolidin-1-yl]methyl]phenoxy]benzamide (26).** To a solution of (2R)-3-fluorophenyl pyrrolidine (1.0 equiv, 0.15 mmol) and 3-fluoro-4-(4-formylphenoxy)benzamide (**24**) (1 equiv, 0.15 mmol) in THF (0.1 mL) was stirred. Dibutyl tin chloride (0.02 equiv, 0.003 mmol) was added, and stirring was continued for 5 min. Phenyl silane (1.1 equiv, 0.16 mmol) was added, and stirring was continued for 4 h. The reaction mixture was subjected to SCX chromatography. The SCX (0.5 g) cartridge was pretreated with 2 volumes of methanol (3 mL). The sample was loaded and eluted with 1 volume of methanol followed by elution with 2N ammonia in methanol. The basic eluent was evaporated to yield the desired final compound. Yield = 80%. The retention time of this compound matches the retention time of the second eluting peak from enantiomers previously separated by preparative chiral HPLC. Chiral HPLC = 98% at 7.221 min by chiral HPLC method 6.

**4-[4-[2-(3,5-Dimethylphenyl)pyrrolidin-1-yl]methyl]phenoxy]-3-fluoro-benzamide (28).** Compound **28** was prepared from **22** using general procedure C. Yield (69%). HPLC = 99% at 2.88 min, mass spectrum ( $m/z$ ): 419.2 ( $M + 1$ ) by HPLC-MS method 2.  $^1\text{H}$  NMR (300.13 MHz, DMSO): 8.03 (s, 1H), 7.86 (dd,  $J = 1.9$ , 12.0 Hz, 1H), 7.72 (d,  $J = 8.4$  Hz, 1H), 7.49 (s, 1H), 7.27 (d,  $J = 8.4$  Hz, 2H), 7.12–6.97 (m, 5H), 6.86 (s, 1H), 3.65 (d,  $J = 13.1$  Hz, 1H), 3.28 (t,  $J = 8.2$  Hz, 1H), 3.04–2.92 (m, 2H), 2.26 (s, 6H), 2.21–2.05 (m, 2H), 1.81–1.65 (m, 2H), 1.64–1.50 (m, 1H).

**4-[4-[(2S)-2-(3,5-Dimethylphenyl)pyrrolidin-1-yl]methyl]phenoxy]-3-fluoro-benzamide (29).** Compound **29** was prepared from **28** using general procedure F. Yield (49%). HPLC = 100% at 2.25 min, mass spectrum ( $m/z$ ): 419.0 ( $M + 1$ ) by HPLC-MS method 2. Chiral HPLC = 99% at 4.6 min by chiral HPLC method 7. Specific rotation =  $[\alpha]_{\text{D}}^{20} -22.28$  ( $c$  1.00, EtOH).

**4-[4-[(2S)-2-(3,5-Dimethylphenyl)pyrrolidin-1-yl]methyl]phenoxy]-3-fluoro-benzamide (29).** Compound **29** was prepared from **27** and (2S)-2-(3,5-dimethylphenyl) pyrrolidine following general procedure F. Yield (50%). The retention time of this compound matches the retention time of the first eluting peak from enantiomers previously separated by preparative chiral HPLC. Chiral HPLC = 99% at 4.6 min by chiral HPLC method 7.

**4-[4-[(2R)-2-(3,5-Dimethylphenyl)pyrrolidin-1-yl]methyl]phenoxy]-3-fluoro-benzamide (30).** Compound **30** was prepared from **28** using general procedure F. Yield (46%). HPLC = 100% at 2.25 min, mass spectrum ( $m/z$ ): 419.0 ( $M + 1$ ) by HPLC-MS method 2. Chiral HPLC = 99% at 8.8 min by chiral HPLC method 7. Specific rotation =  $[\alpha]_{\text{D}}^{20} +21.56$  ( $c$  1.00, EtOH).

**3-Amino-2,2-dimethyl-3-phenyl-propan-1-ol (31).** Compound **31** was prepared from isobutyraldehyde, benzaldehyde and urethane using the procedure from ref 33. The crude product was used in the next step without distillation. HPLC = 90% at 1.59 min by HPLC method 2, mass spectrum ( $m/z$ ): 180.3 ( $M + 1$ ).

**6-[4-[[[(3-Hydroxy-2,2-dimethyl-1-phenyl-propyl)amino]methyl]phenoxy]pyridine-3-carboxamide (32).** Compound **9** (1 equiv, 3.24 mmol, 784 mg) in dioxane (25 mL) was added to a solution of compound **31** (1.0 equiv, 3.24 mmol, 58 mg) in dioxane (75 mL) solution containing concentrated acetic acid (55.28 mmol, 3.17 mL). Silica supported cyanoborohydride (343.55 mmol, 13.00 g) was added to the reaction mix and then placed on a shaker overnight at room temperature. The reaction mixture was filtered, and the filter cake was washed with THF. The filtrate was concentrated, and the residue was dissolved in ethyl acetate which was washed with 1N aqueous sodium hydroxide, brine, dried over sodium sulfate, and then concentrated in vacuo. The resulting crude material was purified by flash chromatography on silica gel eluting with 0–4% (2 M ammonia in methanol) in dichloromethane to afford 745 mg of 6-[4-[[[(3-hydroxy-2,2-dimethyl-1-phenyl-propyl)amino]methyl]phenoxy]pyridine-3-carboxamide. Yield (57%).  $^1\text{H}$  NMR (400.15 MHz, DMSO): 8.58 (d,  $J = 2.6$  Hz, 1H), 8.23 (dd,  $J = 2.4$ , 8.6 Hz, 1H), 8.03–7.97 (m, 1H), 7.48–7.41 (m, 1H), 7.32–7.26 (m, 7H), 7.07–7.01 (m, 3H), 4.96–4.93 (m, 1H), 3.54–3.44 (m, 2H), 3.28–3.19 (m, 3H), 2.93–2.87 (m, 1H), 0.85 (s, 3H), 0.61 (s, 3H).

**6-[4-[(3,3-Dimethyl-2-phenyl-azetidin-1-yl)methyl]phenoxy]pyridine-3-carboxamide (33).** Compound **32** (1.0 equiv, 1.80 mmol, 0.73 g) was dissolved in dichloromethane (40 mL) and cooled to 0  $^{\circ}\text{C}$ , whereupon (bis(2-methoxyethyl)amino)sulfur trifluoride (1.25 equiv, 2.25 mmol, 0.498 g) was added dropwise to the reaction. The reaction was stirred for 5 min, cooled to 0  $^{\circ}\text{C}$ , and then quenched with saturated aqueous sodium bicarbonate. The organic phase was separated, washed consecutively with water and brine, and then concentrated in vacuo to give the crude product. The resulting crude material was purified by flash chromatography on silica gel eluting with 0–4% (2 M ammonia in methanol) in dichloromethane to afford 0.52 g of 6-[4-[(3,3-dimethyl-2-phenyl-azetidin-1-yl)methyl]phenoxy]pyridine-3-carboxamide. Yield (74%). HPLC = 88.8% at 1.78 min by HPLC method 2, mass spectrum ( $m/z$ ): 388 ( $M + 1$ ). Exact mass ( $M + 1$ ): calcd 388.2020; found 388.2011.  $^1\text{H}$  NMR (400.15 MHz, DMSO): 8.59 (d,  $J = 2.2$  Hz, 1H), 8.25–8.21 (m, 1H), 8.03–7.98 (m, 1H), 7.45 (s, 1H), 7.37 (d,  $J = 8.4$  Hz, 2H), 7.32–7.22 (m, 5H), 7.09–7.06 (m, 2H), 6.98 (d,  $J = 8.8$  Hz, 1H), 3.95 (s, 1H), 3.78–3.73 (m, 1H), 3.43 (d,  $J = 13.2$  Hz, 1H), 3.00 (d,  $J = 6.2$  Hz, 1H), 2.70 (d,  $J = 6.2$  Hz, 1H), 1.19 (s, 3H), 0.72 (s, 3H).

**6-[4-[(2R)-3,3-Dimethyl-2-phenyl-azetidin-1-yl]methyl]phenoxy]pyridine-3-carboxamide (34).** Compound **34** was separated from **33** using 8 cm  $\times$  35 cm Chiralcel OJ column, 20  $\mu\text{m}$  eluting with 70/30 MeOH/ACN with 0.2% DMEA, at a flow rate of 400 mL/min. Yield (41.09%), ee >99%. The absolute configuration was assigned based on the comparison of the experimental and theoretical VCD spectra; Chiral HPLC = 99% at 10.4 min by chiral HPLC method 8; HPLC = 100% at 1.69 min by HPLC method 2, mass spectrum ( $m/z$ ): 388 ( $M + 1$ ). Specific rotation =  $[\alpha]_{\text{D}}^{20} +32.96$  ( $c$  1.00, EtOH).  $^1\text{H}$  NMR (400.15 MHz, DMSO): 8.59 (d,  $J = 2.6$  Hz, 1H), 8.24–8.21 (m, 1H), 8.06–7.95 (m, 1H), 7.54–7.48 (m, 1H), 7.37 (d,  $J = 8.4$  Hz, 2H), 7.32–7.22 (m, 5H), 7.08 (m, 2H), 6.98 (d,  $J = 8.8$  Hz, 1H), 3.95 (s, 1H), 3.78–3.74 (m, 1H), 3.43 (d,  $J = 13.2$  Hz, 1H), 3.00 (d,  $J = 6.2$  Hz, 1H), 2.70 (d,  $J = 6.2$  Hz, 1H), 1.19 (s, 3H), 0.72 (s, 3H).

**6-[4-[(2S)-3,3-Dimethyl-2-phenyl-azetidin-1-yl]methyl]phenoxy]pyridine-3-carboxamide (35).** Compound **35** was separated from **33** using 8 cm  $\times$  35 cm Chiralcel OJ column, 20  $\mu\text{m}$  eluting with 70/30 MeOH/ACN with 0.2% DMEA, at a flow rate of 400 mL/min. Yield (42.77%). ee >99%. The absolute configuration was assigned based on the comparison of the experimental and theoretical VCD spectra; chiral HPLC = 99% at 5.3 min by chiral HPLC method 8; HPLC = 89.1% at 1.7 min by HPLC Method 2, mass spectrum ( $m/z$ ): 388 ( $M + 1$ ). Specific rotation =  $[\alpha]_{\text{D}}^{20} -48.23$  ( $c$  1.00, EtOH).  $^1\text{H}$  NMR (400.15 MHz, DMSO): 8.59 (d,  $J = 2.6$  Hz, 1H), 8.24–8.21 (m, 1H), 8.04–7.97 (m, 1H), 7.51–7.42 (m, 1H), 7.37 (d,  $J = 8.4$  Hz, 2H), 7.32–7.22 (m, 5H), 7.09–7.07 (m, 2H), 6.98 (d,  $J = 8.8$  Hz, 1H), 3.95 (s, 1H),



3.78–3.73 (m, 1H), 3.54–3.41 (m, 1H), 3.00 (d,  $J = 6.2$  Hz, 1H), 2.70 (d,  $J = 6.2$  Hz, 1H), 1.19 (s, 3H), 0.72 (s, 3H).

**In Vitro Opioid Receptor Assays.** *Reagents.* Membranes from Chinese hamster ovary (CHO) cells expressing the human  $\mu$  opioid receptor and membranes from human embryonic kidney (HEK) 293 cells expressing the human  $\delta$  opioid receptor were obtained from Perkin-Elmer Life and Analytical Sciences (Boston, MA). A CHO cell line which stably expressed the human  $\kappa$  opioid receptor was generated at Lilly Research Laboratories, and membranes from this cell line were prepared by MDS Pharma (Bothell, WA).

All other reagents were obtained from Sigma Aldrich Chemical Co. (St. Louis, MO) or Invitrogen (Carlsbad, CA) and were analytical grade quality or better.

**Opioid Receptor Binding Assays with [ $^3$ H]-Diprenorphine.** Assays were performed using protocols based upon previously published studies.<sup>21</sup> Compounds were dissolved at 10 mM in 100% DMSO and diluted in buffer (50 mM Tris-HCl, pH 7.4, 5 mM MgCl<sub>2</sub>) and pipetted into a 96-well polypropylene plate. First, 11 point concentration curves (final concentrations of 0.01 nM to 1  $\mu$ M) were prepared in this plate using a Tecan Evo liquid handler. Then 50  $\mu$ L of each dilution and 50  $\mu$ L of [ $^3$ H]diprenorphine (abbreviated as [ $^3$ H]DPN, obtained from Perkin-Elmer Life and Analytical Sciences, NET1121) were added to a polypropylene 96 deep well assay block using a Beckman Multimek 96 channel automated pipettor. The final assay concentration of [ $^3$ H]-DPN was near the  $K_d$  for each receptor ( $\kappa$ , 0.27 nM,  $\mu$ , 0.35 nM,  $\delta$ , 1.5 nM) and was determined for each experiment using total counts added. Reactions were initiated by addition of 100  $\mu$ L of membranes (4–10  $\mu$ g of protein) in buffer (50 mM Tris-HCl, pH 7.4, 5 mM MgCl<sub>2</sub>, 125 mM NaCl, and 200  $\mu$ M GDP) using a Multidrop liquid dispenser. Total binding and nonspecific binding were defined by addition of either buffer (50 mM Tris-HCl, pH 7.4, 5 mM MgCl<sub>2</sub>) or 10  $\mu$ M naltrexone in buffer to a series of four wells on each assay plate. Assay blocks were incubated for 120 min at room temperature (22 °C). Glass fiber filtermats (GF/C Filtermat A, Perkin-Elmer Life and Analytical Sciences) were presoaked in a solution of 50 mM Tris-HCl, pH 7.4 containing 0.3% (w/v) polyethylimine (PEI) for 30 min prior to use. Assays were terminated by filtration through the glass fiber filter mats mounted in a Tomtec Mach III cell harvester and washed three times with 5 mL of ice-cold 50 mM Tris-HCl, pH 7.4 buffer. Filtermats were dried 1–2 h in an oven at 60 °C and embedded with Meltlux A solid scintillant (Perkin-Elmer Life and Analytical Sciences). Radioactivity was determined as counts per minute (CPM) using a Trilux Microbeta plate scintillation counter (Perkin-Elmer Life and Analytical Sciences). A concentration response curve for naltrexone was included on each plate as a quality control check.

Raw CPM data for concentration response curves of each compound were converted to specific percent inhibition by subtracting nonspecific binding (10  $\mu$ M naltrexone control wells) from the individual CPM values and dividing by the maximum uninhibited response, also corrected by subtracting nonspecific binding. Data was analyzed using four-parameter (curve maximum, curve minimum, IC<sub>50</sub>, Hill slope) nonlinear regression routines (XLfit version 4.0; ActivityBase, IDBS), where IC<sub>50</sub> is the concentration of added compound that results in 50% inhibition of [ $^3$ H]DPN binding. The equilibrium dissociation constant ( $K_i$ ) was calculated from the relative IC<sub>50</sub> value based upon the equation  $K_i = \text{IC}_{50}/(1 + L/K_d)$ , where  $L$  equals the concentration of radioligand used in the experiment and  $K_d$  equals the equilibrium binding affinity constant of the radioligand. If a compound did not have at least 50% inhibition at the highest concentration tested, the IC<sub>50</sub> was reported as >1000 nM, which was used in the equation for calculation of the affinity constant ( $K_i$ ).

**GTP- $\gamma$ -S Antagonist Functional Assays.** Assays were conducted in clear bottom 96-well microplates using protocols based upon previously published studies.<sup>22</sup> Reagent dispensing into plates was conducted with Beckman Multimek 96-channel robots and Titertek Multidrops. Stock solutions of test compound or naltrexone were diluted in buffer

(50 HEPES, pH 7.4, 5 mM MgCl<sub>2</sub>) and pipetted into a 96-well polypropylene plate. Then 11 point concentration curves that bracketed the IC<sub>50</sub> (highest final concentration of 1  $\mu$ M or 10  $\mu$ M) were prepared in this plate using a Tecan Evo liquid handler. Membranes were thawed and diluted with assay buffer (20 mM HEPES, pH 7.4, 5 mM MgCl<sub>2</sub>, 100 mM NaCl, 1 mM EDTA, 1 mM dithiothreitol) containing 200  $\mu$ M GDP and homogenized using a Polytron. A GTP- $\gamma$ -<sup>35</sup>S mixture (0.5 nM final) was prepared for each receptor with the addition of an agonist specific for each opioid receptor. For  $\kappa$ , U69,693 was added (300 nM final assay concentration), for  $\mu$ , DAMGO was added (1  $\mu$ M final), and for  $\delta$ , DPDPE was added (30 nM final). The final agonist concentrations are equal to concentrations that stimulate approximately 80% of the maximum GTP- $\gamma$ -S binding in the absence of antagonist. Finally, 50  $\mu$ L of each compound dilution, 50  $\mu$ L of GTP- $\gamma$ -<sup>35</sup>S/agonist solution, 50  $\mu$ L of diluted membranes (15–30  $\mu$ g protein), and 50  $\mu$ L of WGA SPA beads (1 mg) prepared in assay buffer were added to the assay plate in the order listed. Following an incubation of 2 h ( $\delta$ ) or 4 h ( $\kappa$  and  $\mu$ ) at room temperature, the assay plates were placed at 4 °C overnight to allow the SPA beads to settle to the bottom of the well. Radioactivity in the plates was determined using a Trilux Microbeta scintillation counter (Perkin-Elmer Life and Analytical Sciences) and reported in counts per minute (CPM). For total GTP- $\gamma$ -S binding, assay buffer was used in place of added compound. For nonspecific GTP- $\gamma$ -S binding, the following antagonists were used:  $\kappa$  (NorBNI at 10  $\mu$ M final),  $\mu$  (naltrexone at 10  $\mu$ M final), and  $\delta$  (naltriben at 10  $\mu$ M final).

Agonist concentration curves were obtained at each receptor on the day of compound testing in order to generate an EC<sub>50</sub> for calculating antagonist potency. The EC<sub>50</sub>s were determined for U69,693 and DAMGO over a concentration range of 0.1 nM to 10  $\mu$ M and for DPDPE over a concentration range of 0.01 nM to 1  $\mu$ M.

Raw CPM data for concentration response curves of test compound were converted to specific percent inhibition by subtracting nonspecific GTP- $\gamma$ -S binding (10  $\mu$ M NorBNI, naltrexone or naltriben) from the individual CPM values and dividing by the maximum uninhibited response, also corrected by subtracting nonspecific GTP- $\gamma$ -S binding. Data were analyzed using four-parameter (curve maximum, curve minimum, IC<sub>50</sub>, Hill slope) nonlinear regression routines (XLfit version 4.0; ActivityBase, IDBS), where IC<sub>50</sub> is the concentration of added compound that results in 50% inhibition of GTP- $\gamma$ -<sup>35</sup>S binding. The antagonist equilibrium dissociation constant ( $K_b$ ) was calculated from the relative IC<sub>50</sub> value based upon the equation  $K_b = \text{IC}_{50}/(1 + D/\text{EC}_{50})$ , where  $D$  equals the concentration of agonist used in the experiment and EC<sub>50</sub> equals the concentration of the agonist producing one-half maximal stimulation. Reported values for  $K_b$  are shown as geometric mean  $\pm$  the standard error of the mean (SEM), with the number of replicate determinations indicated by  $n$ . Geometric means are calculated by the equation  $\text{GeoMean} = 10(\text{Average}(\log K_{i1} + \log K_{i2} + \dots \log K_{in})/\text{sqrt } n)$ .

**In Vivo Tracer Characterization.** Doses of the potential tracers were selected to be low and still permit accurate measurement by LC/MS/MS. Groups of four rats were injected with a single tracer and sacrificed 20 or 40 min post iv tracer. Striatal and cerebellar levels of tracer were measured by LC/MS/MS. Striatal levels of tracer represent total binding. Cerebellar levels represent nonspecific binding as this tissue region has little to no expression of  $\kappa$ , nor  $\mu$  or  $\delta$  opioid receptors.<sup>27</sup> Specific to nonspecific binding of the tracer was determined by the method of Wadenberg,<sup>26</sup> calculated from

$$((\text{tracer concentration in striatum}/\text{tracer concentration in cerebellum}) - 1$$

Additionally, %SUV (standardized uptake value) was calculated as the proportion of the injected tracer dose reaching the target rich tissue—striatum.

$$\% \text{SUV} = [(\text{Tracer Amt Measured in Tissue})/(\text{Injected Tracer Dose})] \times 100$$

**Tissue Preparation and Analysis for in Vivo Tracer Characterization.** Striatal and cerebellar samples were weighed and placed in conical centrifuge tubes on ice. Four volumes (w/v) of acetonitrile containing 0.1% formic acid was added to each tube. These samples were then homogenized using an ultrasonic probe and centrifuged. Supernatant was diluted with sterile water in HPLC injection vials for LC/MS/MS analysis.

Analysis of potential tracers were carried out using an Agilent model 1200 HPLC (Agilent Technologies, Palo Alto, CA) and an API 4000 mass spectrometer (Applied Biosystems, Foster City, CA, USA). The chromatographic separation employed a 2.1 mm × 50 mm C18 column (Agilent part number 971700-907) and a mobile phase consisting of varying concentrations of acetonitrile dependent on the molecule with an overall 0.1% formic acid content. Detection of all small molecules was accomplished by monitoring the precursor to product ion transition. Standards were prepared by adding known quantities of analyte to brain tissue samples from nontreated rats and processed as described above.

**Computational Chemistry Methods.** Several models used in this analysis were generated using data from an internal brain exposure assessment (BEA) suite of assays.<sup>30</sup> Brain-to-plasma ratio (regression) models were built using recursive partitioning methodology (with bagging<sup>31</sup>) and internally generated data for both end points. The unbound fraction models (i.e., brain and plasma; regression) were built using support vector machine (SVM)<sup>32</sup> methods employing a fingerprint-based Tanimoto similarity kernel. Validation for these models was done using a true prospective test set.

## ■ ASSOCIATED CONTENT

**S Supporting Information.** Information on the assignment of absolute configuration for 2-(3,5-dimethylphenyl)pyrrolidine based on preparation of its corresponding Mosher amide and NMR analysis of the Mosher amide derivative. Measured and calculated vibrational circular dichroism spectra used for the assignment of absolute configuration for compounds **34** and **35**. This material is available free of charge via the Internet at <http://pubs.acs.org>.

## ■ AUTHOR INFORMATION

### Corresponding Author

\*Phone: (317) 276-3148. E-mail: [mitch@lilly.com](mailto:mitch@lilly.com).

## ■ ABBREVIATIONS USED

CHO, Chinese hamster ovary; DAMGO, L-tyrosyl-D-alanylglycyl-N-(2-hydroxyethyl)-N $\alpha$ -methyl-L-phenylalaninamide; DPDPE, L-tyrosyl-3-mercapto-D-valylglycyl-L-phenylalanyl-3-mercapto-, cyclic (2S)-disulfide, D-valine; fu-brain, fraction unbound in brain; GDP, guanosine diphosphate; [<sup>35</sup>S]-GTP- $\gamma$ -S, [<sup>35</sup>S]-guanosine 5'-O-[3-thiotriphosphate]; LC/MS/MS, liquid chromatography–tandem mass spectrometry; %SUV, percent standardized uptake value; PET, positron emission tomography; SPA, scintillation proximity assay; U69,593, N-methyl-N-[(5R,7S,8S)-7-(1-pyrrolidinyl)-1-oxaspiro[4.5]dec-8-yl]-benzeneacetamide; VCD, vibrational circular dichroism

## ■ REFERENCES

- (1) Martin, W. R.; Eades, C. G.; Thompson, J. A.; Huppler, R. E.; Gilbert, P. E. The Effects of Morphine- and Nalorphine- Like Drugs in the Nondependent and Morphine-Dependent Chronic Spinal Dog. *J. Pharmacol. Exp. Ther.* **1976**, *197*, 517–532.
- (2) (a) Chavkin, C.; James, I. F.; Goldstein, A. Dynorphin Is a Specific Endogenous Ligand of the Kappa Opioid Receptor. *Science*

**1982**, *215*, 413–415. (b) Schwarzer, C. 30 Years of Dynorphins—New Insights on Their Functions in Neuropsychiatric Diseases. *Pharmacol. Ther.* **2009**, *123*, 353–370.

- (3) Szmuskovicz, J.; Von Voigtlander, P. F. Benzeneacetamide Amines: Structurally Novel Non-Mu Opioids. *J. Med. Chem.* **1982**, *25*, 1125–1126.

- (4) Pfeifer, A.; Brantl, V.; Herz, A.; Emrich, H. M. Psychotomimesis Mediated by  $\kappa$  Opiate Receptors. *Science* **1986**, *233*, 774–776.

- (5) Spanagel, R.; Herz, A.; Shippenberg, T. S. The Effects of Opioid Peptides on Dopamine Release in the Nucleus Accumbens: an in Vivo Microdialysis Study. *J. Neurochem.* **1990**, *55*, 1734–1740.

- (6) Yasuda, K.; Raynor, K.; Kong, H.; Breder, C. D.; Takeda, J.; Reisine, T.; Bell, G. I. Cloning and Functional Comparison of Kappa and Delta Opioid Receptors from Mouse Brain. *Proc. Natl. Acad. Sci. U.S.A.* **1993**, *90*, 6736–6740.

- (7) Mansson, E.; Bare, L.; Yang, D. Isolation of a Human Kappa Opioid Receptor cDNA from Placenta. *Biochem. Biophys. Res. Commun.* **1994**, *202*, 1431–1437.

- (8) (a) Chen, Y.; Mestek, A.; Liu, J.; Yu, L. Molecular Cloning of a Rat Kappa Opioid Receptor Reveals Sequence Similarities to the Mu and Delta Opioid Receptors. *Biochem. J.* **1993**, *295*, 625–628. (b) Filizola, M.; Carteni-Farina, M.; Perez, J. J. Molecular Modeling Study of the Differential Ligand–Receptor Interaction at the Mu, Delta and Kappa Receptors. *J. Comput.-Aided Mol. Des.* **1999**, *13*, 397–407.

- (9) Metcalf, M. D.; Coop, A. Kappa Opioid Antagonists: Past Successes and Future Prospects. *AAPS J.* **2005**, *7*, E704–E722.

- (10) Nutt, D.; Groves, S.; Coupland, N.; Glue, P. Buprenorphine in Psychiatric Disorders. In *Buprenorphine: Combatting Drug Abuse with a Unique Opioid*; Cowan, A.; Lewis, J. W., Eds.; Wiley-Liss, Inc.: New York, 1995; pp 175–186.

- (11) Mague, S. D.; Pliakas, A. M.; Todtenkopf, M. S.; Tomasiewicz, H. C.; Zhang, Y.; Stevens, W. C.; Jones, R. M.; Portoghese, P. S.; Carlezon, W. A. Antidepressant-Like Effects of Kappa Opioid Receptor Antagonists in the Forced Swim Test in Rats. *J. Pharmacol. Exp. Ther.* **2003**, *305*, 323–330.

- (12) Kuzmin, A. V.; Gerrits, A. F. M.; Van Ree, J. M. Kappa-Opioid Receptor Blockade with nor-Binaltorphimine Modulates Cocaine Self-Administration in Drug-Naïve Rats. *Eur. J. Pharmacol.* **1998**, *358*, 197–202.

- (13) (a) Portoghese, P. S.; Lipkowski, A. W.; Takemori, A. E. Bimorphinans as Highly Selective, Potent Kappa Opioid Receptor Antagonists. *J. Med. Chem.* **1987**, *30*, 238–239. (b) Takemori, A. E.; Ho, B. Y.; Naeseth, J. S.; Portoghese, P. S. nor-Binaltorphimine, a Highly Selective Kappa-Opioid Antagonist in Analgesic and Receptor Binding Assays. *J. Pharmacol. Exp. Ther.* **1988**, *246*, 255–258.

- (14) Thomas, J. B.; Atkinson, R. N.; Vinson, N. A.; Catanzaro, J. L.; Perretta, C. L.; Fix, S. E.; Mascarella, S. W.; Rothman, R. B.; Xu, H.; Dersch, C.; Cantrell, B. E.; Zimmerman, D. M.; Carroll, F. I. Identification of (3R)-7-Hydroxy-N-((1S)-1-([3R,4R]-4-(3-hydroxyphenyl)-3,4-dimethyl-1-piperidinyl)methyl)-2-methylpropyl)-1,2,3,4-tetrahydro-3-isoquinolinecarboxamide as a Novel Potent and Selective Opioid Kappa Receptor Antagonist. *J. Med. Chem.* **2003**, *46*, 3127–3137.

- (15) (a) Brugel, T. A.; Smith, R. W.; Balestra, M.; Becker, C.; Daniels, T.; Hoerter, T. N.; Koether, G. M.; Throner, S. R.; Panko, L. M.; Folmer, J. J.; Cacciola, J.; Hunter, A. M.; Liu, R.; Edwards, P. D.; Brown, D. G.; Gordon, J.; Ledonne, N. C.; Pietras, M.; Schroeder, P.; Sygowski, L. A.; Hirata, L. T.; Zacco, A.; Peters, M. F. Discovery of 8-Azabicyclo[3.2.1]octan-3-yloxy-benzamides as Selective Antagonists of the Kappa Opioid Receptor. Part 1. *Bioorg. Med. Chem. Lett.* **2010**, *20*, 5847–5852. (b) Brugel, T. A.; Smith, R. W.; Balestra, M.; Becker, C.; Daniels, T.; Koether, G. M.; Throner, S. R.; Panko, L. M.; Brown, D. G.; Liu, R.; Gordon, J.; Peters, M. F. SAR Development of a Series of 8-azabicyclo[3.2.1]octan-3-yloxy-benzamides as Kappa Opioid Receptor Antagonists. Part 2. *Bioorg. Med. Chem. Lett.* **2010**, *20*, 5405–5410.

- (16) Talbot, P. S.; Narendran, R.; Butelman, E. R.; Huang, Y.; Ngo, K.; Slifstein, M.; Martinez, D.; Laruelle, M.; Hwang, D. <sup>11</sup>C-GR103545, a Radiotracer for Imaging Kappa-Opioid Receptors in Vivo with PET: Synthesis and Evaluation in Baboons. *J. Nucl. Med.* **2005**, *46*, 484–494.



- (17) (a) Takeuchi, K.; Holloway, W. G.; McKinzie, J. H.; Suter, T. M.; Statnick, M. A.; Surface, P. L.; Emmerson, P. J.; Thomas, E. M.; Siegel, M. G.; Matt, J. E.; Wolfe, C. N.; Mitch, C. H. Structure–activity relationship studies of carboxamido-biaryl ethers as opioid receptor antagonists (OpRAs). Part 1. *Bioorg. Med. Chem. Lett.* **2007**, *17*, 5349–5352. (b) Takeuchi, K.; Holloway, W. G.; Mitch, C. H.; Quimby, S. J.; McKinzie, J. H.; Suter, T. M.; Statnick, M. A.; Surface, P. L.; Emmerson, P. J.; Thomas, E. M.; Siegel, M. G. Structure–activity relationship studies of carboxamido-biaryl ethers as opioid receptor antagonists (OpRAs). Part 2. *Bioorg. Med. Chem. Lett.* **2007**, *17*, 6841–6846.
- (18) Vidal, P.; Pedregal, C.; Diaz, N.; Broughton, H.; Acena, J. L.; Jimenez, A.; Espinosa, J. F. Assignment of Absolute Configuration on the Basis of the Conformational Effects Induced by Chiral Derivatizing Agents: The 2-Arylpyrrolidine Case. *Org. Lett.* **2007**, *9*, 4123–4126.
- (19) Stephens, P. J.; Devlin, F. J.; Pan, J. J. The Determination of the Absolute Configurations of Chiral Molecules Using Vibrational Circular Dichroism (VCD) Spectroscopy. *Chirality* **2008**, *20*, 643–663.
- (20) Seeman, J. I.; Chavdarian, C. G.; Secor, H. V. Synthesis of the Enantiomers of Nornicotine. *J. Org. Chem.* **1985**, *50*, 5419–5421.
- (21) Emmerson, P. J.; McKinzie, J. H.; Surface, P. L.; Suter, T. M.; Mitch, C. H.; Statnick, M. A. Na<sup>+</sup> Modulation, Inverse Agonism, and Anorectic Potency of 4-Phenylpiperidine Opioid Antagonists. *Eur. J. Pharmacol.* **2004**, *494*, 121–130.
- (22) Rodgers, G.; Hubert, C.; McKinzie, J.; Suter, T.; Statnick, M.; Emmerson, P.; Stancato, L. Development of Displacement Binding and GTP-gamma-S Scintillation Proximity Assays for the Identification of Antagonists of the Mu Opioid Receptor. *Assay Drug Dev. Technol.* **2003**, *1*, 627–636.
- (23) Shannon, H. E.; Lutz, E. A. Comparison of the Central and Peripheral Effects of the Opioid Agonists Loperamide and Morphine in the Formalin Test in Rats. *Neuropharmacology* **2002**, *42*, 253–261.
- (24) (a) Chernet, E.; Martin, L. J.; Li, D.; Need, A. B.; Barth, V. N.; Rash, K. S.; Phebus, L. A. Use of LC/MS to Assess Brain Tracer Distribution in Preclinical, in Vivo Receptor Occupancy Studies: Dopamine D<sub>2</sub>, Serotonin 2A and NK-1 Receptors as Examples. *Life Sci.* **2005**, *78*, 340–346. (b) Need, A. B.; McKinzie, J. H.; Mitch, C. H.; Statnick, M. A.; Phebus, L. A. In Vivo Rat Brain Opioid Receptor Binding of LY255582 Assessed with a Novel Method Using LC/MS/MS and the Administration of Three Tracers Simultaneously. *Life Sci.* **2007**, *81*, 1389–1396.
- (25) (a) Akil, H.; Meng, F.; Thompson, R.; Mansour, A.; Xie, G. X.; Watson, S. J. Molecular Studies of Multiple Opioid Receptors: Cloning, Anatomical Distribution, Pharmacological Profile. *Regul. Pept.* **1994**, No. Suppl. 1, S9–S10. (b) Mansour, A.; Fox, C. A.; Burke, S.; Watson, S. J. Immunohistochemical Localization of the Kappa Opioid Receptors. *Regul. Pept.* **1994**, *54*, 177–178. (c) Mansour, A.; Fox, C. A.; Burke, S.; Watson, S. J. Immunohistochemical Localization of the Mu Opioid Receptors. *Regul. Pept.* **1994**, *54*, 179–180.
- (26) Wadenberg, M.; Kapur, S.; Soliman, A.; Jones, C.; Vaccarino, F. Dopamine D<sub>2</sub> Receptor Occupancy Predicts Catalepsy and the Suppression of Conditioned Avoidance Response Behavior in Rats. *Psychopharmacology* **2000**, *150*, 422–429.
- (27) Tempel, A.; Zukin, R. S. Neuroanatomical Patterns of the Mu, Delta and Kappa Opioid Receptors of Rat Brain as Determined by Quantitative In Vitro Autoradiography. *Proc. Natl. Acad. Sci. U.S.A.* **1987**, *84*, 4308–4312.
- (28) Bruchas, M. R.; Yang, T.; Schreiber, S.; DeFino, M.; Kwan, S. C.; Li, S.; Chavkin, C. Long-Acting Kappa Opioid Antagonists Disrupt Receptor Signaling and Produce Noncompetitive Effects by Activating c-Jun N-terminal Kinase. *J. Biol. Chem.* **2007**, *282*, 29803–29811.
- (29) Waterhouse, R. N. Determination of Lipophilicity and Its Use as a Predictor of Blood–Brain Barrier Penetration of Molecular Imaging Agents. *Mol. Imaging Biol.* **2003**, *5*, 376–389.
- (30) Raub, T. J.; Lutzke, B. S.; Andrus, P. K.; Sawada, G. A.; Staton, B. A. Early Preclinical Evaluation of Brain Exposure in Support of Hit Identification and Lead Optimization. In: *Optimizing the “Drug-Like” Properties of Leads in Discovery*, Biotechnology: Pharmaceutical Aspects Series; Borchardt, R. T., Kerns, E. H., Hageman, M. J., Thakker, D. R., Stevens, J. L., Eds.; Springer: New York, 2006; pp 355–410.
- (31) Breiman, L. Bagging Predictors. *Machine Learn.* **1996**, *24*, 123–140.
- (32) Ivanciuc, O. Applications of Support Vector Machines in Chemistry. In: *Reviews in Computational Chemistry*; Lipkowitz, K. B., Cundari, T. R., Eds.; Wiley-VCH: Weinheim, Germany, 2007; pp 291–400.
- (33) ten Hoeve, W.; Wynberg, H. Direct Amidoalkylation of Ketones. *Synth. Commun.* **1994**, *24*, 899–906.